

# Community Workflows to Advance Reproducibility in Hydrologic Modeling: Separating model-agnostic and model-specific configuration steps in applications of large-domain hydrologic models

W. J. M. Knoben<sup>1</sup>, M. P. Clark<sup>1,2</sup>, J. Bales<sup>3</sup>, A. Bennett<sup>4</sup>, S. Gharari<sup>5</sup>, C. B. Marsh<sup>5</sup>, B. Nijssen<sup>6</sup>, A. Pietroniro<sup>7</sup>, R. J. Spiteri<sup>8</sup>, D. G. Tarboton<sup>9</sup>, A. W. Wood<sup>10</sup>

<sup>1</sup>Centre for Hydrology, University of Saskatchewan, Canmore, Alberta, Canada

<sup>2</sup>Department of Geography and Planning, University of Saskatchewan, Saskatoon, Saskatchewan, Canada

<sup>3</sup>Consortium of Universities for the Advancement of Hydrologic Science, Inc, Cambridge, Massachusetts,

USA

<sup>4</sup>Hydrology & Atmospheric Sciences, University of Arizona, Tucson, Arizona, USA

<sup>5</sup>Centre for Hydrology, University of Saskatchewan, Saskatoon, Saskatchewan, Canada

<sup>6</sup>Civil and Environmental Engineering, University of Washington, Seattle, Washington, USA

<sup>7</sup>Schulich School of Engineering, Department of Civil Engineering, University of Calgary, Calgary,

Alberta, Canada

<sup>8</sup>Department of Computer Science, University of Saskatchewan, Saskatoon, Saskatchewan, Canada

<sup>9</sup>Utah Water Research Laboratory, Utah State University, Logan, Utah, USA

<sup>10</sup>National Center for Atmospheric Research, Boulder, Colorado, USA

## Key Points:

- Reproducible, transparent modeling increases confidence in model simulations and requires careful tracking of all model configuration steps
- We show an example of globally applicable model configuration code that is traced and shared through a version control system
- Standardizing file formats and sharing of code can increase community-wide efficiency and reproducibility of modeling studies

---

Corresponding author: W. J. M. Knoben, [wouter.knoben@usask.ca](mailto:wouter.knoben@usask.ca)

## Abstract

Despite the proliferation of computer-based research on hydrology and water resources, such research is typically poorly reproducible. Published studies have low reproducibility because of both incomplete availability of the digital artifacts of research and a lack of documentation on workflow processes. This leads to a lack of transparency and efficiency because existing code can neither be checked nor re-used. Given the high-level commonalities between existing process-based hydrological models in terms of their input data and required pre-processing steps, more open sharing of code can lead to large efficiency gains for the modeling community. Here we present a model configuration workflow that provides full reproducibility of the resulting model instantiation in a way that separates the model-agnostic preprocessing of specific datasets from the model-specific requirements that specific models impose on their input files. We use this workflow to create both a continental and a local setup of the Structure for Unifying Multiple Modeling Alternatives (SUMMA) framework connected to the mizuRoute routing model. These examples show how a relatively complex model setup over a large domain can be organized in a reproducible and structured way that has the potential to accelerate hydrologic modeling for the community as a whole. We provide a tentative blueprint of how a community modeling paradigm can be built on top of workflows such as this. We term this initiative the “Community Workflows to Advance Reproducibility in Hydrologic Modeling” (CWARHM; pronounced “swarm”).

## 1 Introduction

Confidence in published findings depends on the reproducibility of the study. In much of the recent Earth System sciences research, reproducibility requires knowledge of the computer code and data that underpin a given manuscript. Such code can range from a few lines of code that are used to turn data into figures, or compute certain statistical properties of the data, to modern process-based hydrologic models that can contain many thousands of lines of code. Despite encouraging progress in journal policies (Blöschl et al., 2014; Clark et al., 2021a), it is still difficult to reproduce published findings in the hydrologic sciences (Hutton et al., 2016; Stagge et al., 2019). Stagge et al. (2019) estimate that results may only be reproducible for between 0.6% to 6.8% of nearly 2000 peer-reviewed manuscripts in these fields, because of a lack of sufficiently clearly described methods and a lack of the necessary input data or processing code.

In complex process-based hydrologic model applications, one additional barrier to reproducibility is the effort required to configure the model. It is not uncommon to hear claims that in such modeling studies 80% of overall effort is spent on configuring the model for a specific use case, and only 20% on using the model to answer research questions (e.g. Table 2.8 in Miles, 2014). The effort on model configuration is spent on assembling appropriate data sources for meteorological forcing data and geospatial parameter fields, wrangling these data into the specific format required by the model, defining appropriate model settings, and specifying the required computational infrastructure (e.g., finding the right collection of packages and modules, installing the model, creating the required scripts to run the model). Additional time costs are in dealing with the subjectivity in defining appropriate computational sub-domains (such as where to draw the boundaries for Hydrologic Response Units), interpreting soil and land cover maps, aggregating geospatial data into some form of representative value for a computational unit, and the associated iterative model configuration and testing steps. This process is typically poorly documented and - equally important for reproducibility - extremely time-consuming. In short, the reproducibility problem for process-based hydrologists is made worse by a lack of efficiency in model setup tasks.

Recommended best practices for open, accessible, and reproducible science (e.g. Gil et al., 2016; Hutton et al., 2016; Sandve et al., 2013; Stodden and Miguez, 2013) describe

78 how to improve the reproducibility of computational science. Most focus is currently on  
79 advancing the FAIR principles, which state that data, code, and methods must be Find-  
80 able, Accessible, Interoperable, and Reusable (Wilkinson et al., 2016). Reproducibility  
81 requires FAIR data, but also includes sharing details about hardware, software versions,  
82 and data versions (Añel, 2017; Bast, 2019; Hut et al., 2017; Sandve et al., 2013). The  
83 environmental modeling community is interacting with these prescribed best practices  
84 in multiple ways. Choi et al. (2021) identify three ongoing main thrusts aimed at mak-  
85 ing computational environmental science more open, reusable, and reproducible. First,  
86 data and models are increasingly openly available online through services as GitHub, Hy-  
87 droshare, and institutional repositories. Second, computational environments are increas-  
88 ingly recorded and standardized through container applications such as Docker or in self-  
89 documenting notebooks. Third, Application Programming Interfaces (APIs) such as the  
90 pySUMMA API from Choi et al. (2021) make interacting with complex models or data  
91 increasingly easier.

92 Comparatively little attention is devoted to efficient reproducibility of the full mod-  
93 eling workflow, which includes data acquisition, data preprocessing, model installation  
94 model runs and post-processing of simulations. Efficiency is promoted in a general sense  
95 through freely shared code and packages that perform specific tasks in the modeling chain  
96 (for example, see Slater et al., 2019, for an overview of R packages that can be used to  
97 populate a modeling workflow). However, dedicated efforts to ensure end-to-end repro-  
98 ducibility of modeling studies are less common. Exceptions are Leonard & Duffy (2013,  
99 2014, 2016), who provide an in-depth description of a web-based interface for data pre-  
100 processing and visualization of simulations from the PIHM model, geographically con-  
101 strained to the United States; Havens et al. (2020), who provide an end-to-end work-  
102 flow for setting up, running, and analyzing a physics-based snow model; and Vorobevskii  
103 et al. (2020), who develop an R package that sets up a simple hydrologic model anywhere  
104 on the planet for a given domain discretization shapefile provided by the user. Compared  
105 to sharing a model’s input and output data (which would also enable a study to be re-  
106 produced), sharing complete workflows can be more efficient in terms of required stor-  
107 age space. A workflow also provides a transparent record of all modeling decisions, and,  
108 more importantly, having a workflow enables a more broadly defined form of reproducibil-  
109 ity in which a study can be repeated for a different region, a different data set, or a dif-  
110 ferent version of the same model to see if the original conclusions still hold.

111 The examples mentioned in the previous paragraph show that it is possible to doc-  
112 ument workflows for a specific model (or, perhaps more accurately, for a specific version  
113 of a model). A further challenge is in designing workflows in such a way that parts of  
114 a workflow that configures Model A can be re-used in a workflow that configures Model  
115 B. We refer to such a design as separating the model-specific and model-agnostic parts  
116 of model configuration (see also Miles and Band, 2015; Miles, 2014, for an example of  
117 this concept for geospatial data preparation in the field of ecohydrology). In the case of  
118 process-based hydrologic modeling, models such as VIC (Hamman et al., 2018; Liang et  
119 al., 1994), MESH (Pietroniro et al., 2007), SUMMA (Clark et al., 2015a, 2015b, 2021c)  
120 and SVS (Husain et al., 2016) can be different in how they discretize the modeling do-  
121 main, the physical processes they include, and the equations used to describe a given pro-  
122 cess. However, at their core, these models are designed to solve the same general water  
123 and energy conversation equations (Clark et al., 2021c). This means that the data re-  
124 quirements for a myriad of extant hydrologic models will vary in the specifics, but are  
125 similar in a general sense and include, for example, similar needs for meteorological forc-  
126 ing data and geospatial parameter fields. Preprocessing of these similar data requirements  
127 does not need to rely on specifics of the models themselves. For example, in the case of  
128 satellite-based MODIS land cover data (details in Appendix A), model-agnostic steps  
129 are (1) downloading the source data, (2) stitching the source data together into a coher-  
130 ent global map, (3) projecting this map into the Coordinate Reference System of inter-  
131 est, (4) subsetting from the global data only the domain of interest, and (5) mapping

132 the resulting data in pixels onto model elements. Model-specific steps would be to con-  
133 vert the resulting information (i.e., which pixels/land classes are present per model el-  
134 element) to the specific format a model requires (e.g., the mode of the land class per model  
135 element or a distribution of land classes per grid cell), and, if necessary, perform some  
136 form of data transformation to connect land class data to model parameter values or set-  
137 tings. Community-wide efficiency gains are possible if workflows distinguish between model-  
138 agnostic and model-specific steps and enable straightforward re-use of the workflow for  
139 model-agnostic steps (see also Essawy et al., 2016; Gichamo et al., 2020, who makes this  
140 argument in the context of web-based model configuration tools).

141 The hydrologic modeling community is currently not yet at a stage where model  
142 configuration code can easily be shared between modeling groups. Model physics code  
143 is increasingly distributed under open-source licenses, but the code that creates the nec-  
144 essary model inputs is typically neither well-documented nor available without contact-  
145 ing the model developers. To move towards a culture of community Earth System mod-  
146 eling, we define three distinct elements:

- 147 1. For a given model, model configuration code should be publicly available and di-  
148 vided into model-agnostic and model-specific steps;
- 149 2. The configuration workflows of multiple different models, ideally using different  
150 data sets, should be integrated into a proof-of-concept of a generalized model con-  
151 figuration workflow;
- 152 3. A community-wide collaborative effort should refine the proof-of-concept into a  
153 flexible model configuration framework.

154 This paper introduces an open-source model configuration workflow that enables  
155 full reproducibility of a process-based hydrologic model setup for any location on the planet.  
156 The goals of this workflow and the associated code repository are twofold. Our first goal  
157 is to provide an example of open source model configuration code that is divided into  
158 model-agnostic and model-specific steps. This advances our long-term goal of fostering  
159 a community modeling culture within Earth System sciences, where freely shared model  
160 configuration code provides efficiency gains for the modeling community at large. Our  
161 second goal is to provide a traceable and efficient basis from which our chosen model con-  
162 figuration can be used. This advances our short-term goal of using this model configu-  
163 ration for a variety of projects by reducing the time commitment needed to create model  
164 configurations for different domains and by increasing confidence in the modeling out-  
165 comes due to increased transparency and the possibility to reproduce results.

166 In this paper, we configure models that have traditionally been developed for lo-  
167 cal or regional use at high spatial and temporal resolutions across large spatial domains  
168 using a newly developed workflow that distinguishes between model-agnostic and model-  
169 specific configuration steps. In Section 2, we outline several high-level design consider-  
170 ations for model-agnostic workflows. We then use these guidelines to create an exam-  
171 ple implementation of such a workflow using open-source input data with global cover-  
172 age, an open-source, spatially distributed, physics-based hydrologic modeling framework  
173 designed to isolate individual modeling decisions (Clark et al., 2015a, 2015b, SUMMA;  
174 2021c), and an open-source network routing model (mizuRoute; Mizukami et al., 2021,  
175 2016) to generate hydrologic simulations across multiple spatial scales. Technical details  
176 about the models and workflow code are given in Appendix A and B. In Section 3, we  
177 present two test cases, covering continental and local-scale model configurations. In Sec-  
178 tion 4, we reflect on the current state of reproducibility in large-scale hydrologic mod-  
179 eling, with particular focus on why existing efforts have seen only limited uptake and out-  
180 line a path forward.

## 2 Increasing efficiency and reproducibility in Earth System modeling

In this section, we propose general guidelines for model configuration workflows in the Earth System sciences. These guidelines are informed by existing efforts to promote reproducibility and efficiency in large-domain modeling efforts, and by our own experience with creating continental domain model configurations for process-based hydrologic models. We consider challenges for novice and advanced modelers. Briefly, our recommendations are as follows:

1. **Separate model-agnostic and model-specific tasks.** The steps in the workflow must remain model-agnostic for as long as possible and provide outputs in commonly used data formats. This increases the potential utility of the code base for use in different projects and for users of different models.
2. **Clarity for modelers.** The workflow must be easily accessible and useable in its default form. A clear structure of the code accompanied by accurate documentation and in-line comments increase the ease-of-use for novice and advanced modelers alike.
3. **Modularity encourages use beyond the original application.** Customization of the workflow must be possible and easy. This makes it possible to adapt, improve, or change specific parts of the workflow to access new data sets, use new processing algorithms, or target different models.
4. **Traceability is key.** Every outcome of each step in the workflow must be accompanied by metadata that describe the configuration code that generated the outcome. This guarantees that, even if changes are made to the model configuration code, any workflow outcome can still be traced back to its original settings.

These considerations inform the general design of our workflow for setting up a large-scale process-based hydrologic and routing model (sections 2.1-2.4). The workflow starts from a user-provided basin mask that defines the area of interest as discrete modeling elements (e.g., grid cells, sub-basins). Such a mask may be derived from digital elevation models (see e.g. TauDEM (Sazib, 2016; Tesfa et al., 2011) or the geospatialtools code base (Chaney and Fisher, 2021)) or obtained from existing basin masks such as HydroBASINS (Lehner and Grill, 2013) or the MERIT Hydro basin delineation (Lin et al., 2019). The scope of our workflow (Figure 1) includes installation of our chosen hydrologic and routing models, pre-processing of forcing and geospatial parameter data, creation of settings files for both models, model runs, and basic visualization of the resulting model simulations.

Our workflow does not extend to the fine-tuning of parameter values through calibration or estimation from auxiliary data sources, which would necessitate synthesizing several decades of research. A wide variety of calibration algorithms exists, each with their own strengths and weaknesses (Arsenault et al., 2014). These are combined with an even wider variety of objective functions that express the (mis)match between a model's simulations and observations of hydrologic states and fluxes (e.g. Murphy, 1988; Clark et al., 2021b; Gupta et al., 2008; McMillan, 2021; Mizukami et al., 2019; Nash and Sutcliffe, 1970; Olden and Poff, 2003; Pushpalatha et al., 2012), using a variety of further choices related to spatial scaling (e.g. Samaniego et al., 2010), regionalization (e.g. Bock et al., 2015) and dimensionality of the calibration problem (e.g. Pechlivanidis et al., 2011). These choices are not easily standardized and require auxiliary data in the form of observations. Inclusion of calibration and parameter estimation methods is therefore planned for future work in an attempt to keep the scope of this first workflow example manageable.

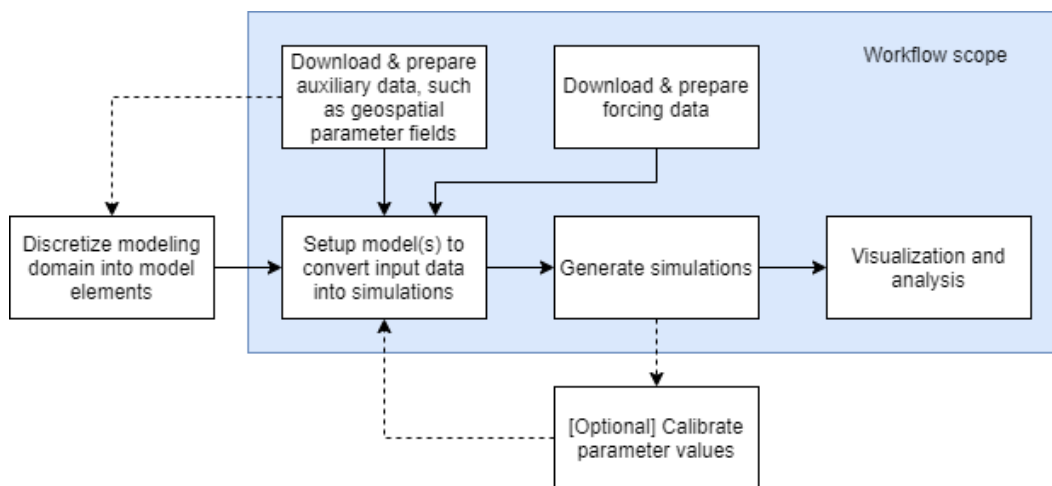


**Figure 1.** Schematic overview of typical modeling workflow. Scope of the example workflow described in this paper shown in blue. Dashed lines indicate potential connections between elements (such as geospatial parameter fields informing basin discretization) that are not included as part of our workflow.

229

## 2.1 Separation of model-agnostic and model-specific tasks

230

231

232

233

234

235

236

Our first design principle recommends separating model-agnostic and model-specific tasks. Figure 2 shows a high-level overview of model configuration tasks and their connections for the process-based hydrologic model and routing model we use in this paper, and how these can be divided into model-agnostic and model-specific tasks. A detailed overview of model-agnostic and model-specific tasks can be found in Figure 3 and Figure 4 respectively. Despite the seemingly large number of model-specific tasks, time costs (in terms of code development) lean heavily towards the model-agnostic tasks.

237

238

239

240

241

242

243

244

245

246

Model-agnostic tasks are those tasks that are the same regardless of the model being used, provided that the model requires a given data input (shown in light grey in Figure 2 and Figure 3). In this example, these tasks include the downloading of meteorological forcing data and geospatial parameter fields (digital elevation model (DEM); soil classes and vegetation classes), in some cases clipping raw datasets to the domain of interest (especially if the raw datasets have a global extent) and mapping of these data onto model elements such as grid cells or catchments. Fully model-agnostic outputs in this example are netCDF files of meteorological forcing data (i.e., gridded hourly data at  $0.25^\circ$  latitude/longitude resolution) and GeoTIFF (.tif) files of several geospatial parameter fields.

247

248

249

250

251

252

Model-specific tasks (shown in dark grey in Figure 2 and Figure 4) involve installing the chosen models, transforming the pre-processed data into the specific format the model requires, and running the models. In our workflow implementation, this involves finding the mean elevation, mode land class and mode soil class per model element and exporting the information about the modeling elements (area, latitude and longitude location, slope of the river network, etc.) into the netCDF files our models expect.

253

254

255

256

257

Due to the complex nature of existing models and their long histories of development, certain tasks cannot be cleanly separated into model-agnostic and model-specific tasks. The mapping of prepared forcing data and geospatial parameter fields onto model elements (shown in the intermediate grey shade in Figure 2 and Figure 3) is an example of such a task. Certain models run on the same resolution as the forcing/data grid

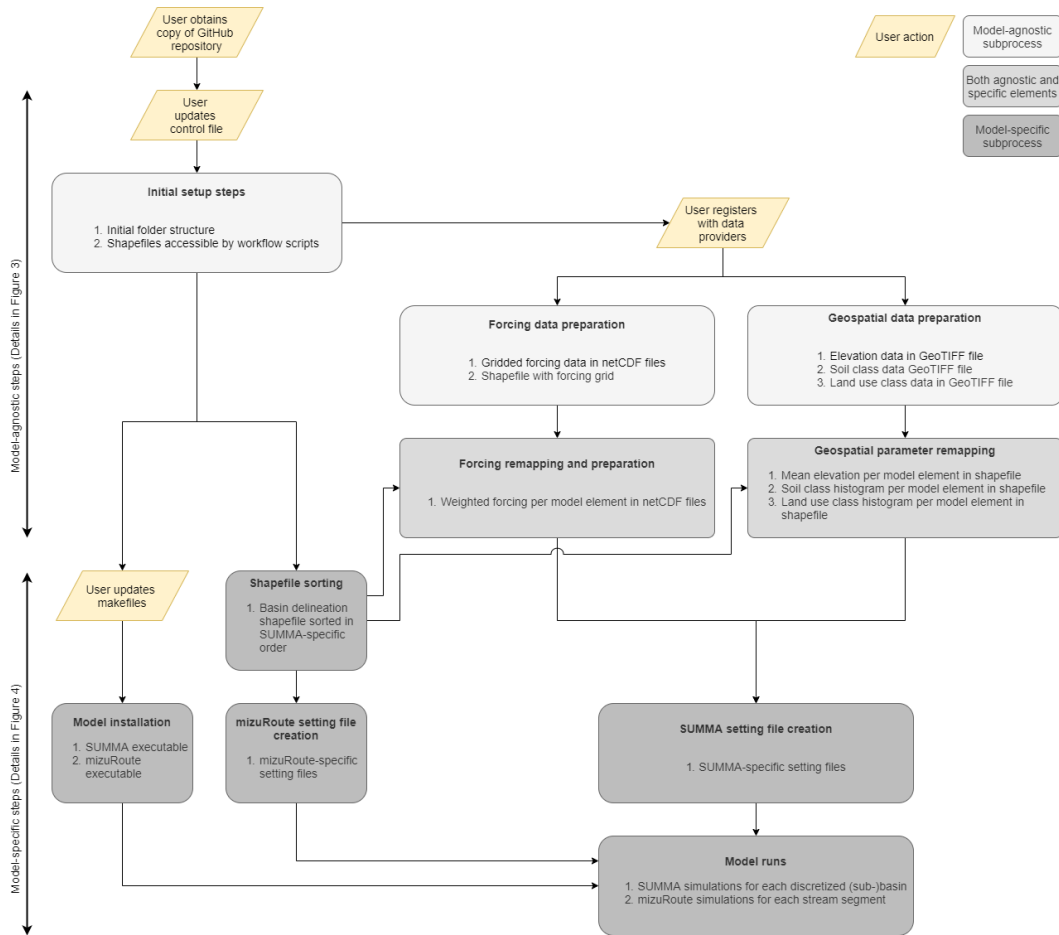


**Figure 2.** High-level overview of model configuration steps, using SUMMA (a process-based hydrologic model) and mizuRoute (a routing model) as example models. Configuration tasks are separated into model-agnostic and model-specific tasks (details in Figure 3 and Figure 4 respectively). Each rounded box specifies the outcomes of that configuration task as a numbered list.

258 or are able to ingest gridded data in their native alignment and internally map these onto  
 259 the required model discretization. In our case, this remapping must be done outside the  
 260 models. In the case of forcing data, the model-agnostic output of meteorological forcing  
 261 files (named “forcing\_yyyymm.nc” in Figure 3) are mapped onto the model elements  
 262 (catchments in this case), resulting in catchment-averaged model forcing. Temperature  
 263 time series are further modified with catchment-specific lapse rates to account for ele-  
 264 vation differences between the forcing grid and model elements. In the case of param-  
 265 eter fields, intersections between the model-agnostic GeoTIFF files and the shapefile of  
 266 the modeling domain are generated. These intersections show how often each elevation  
 267 level, soil class, and land class occurs in each model element. These processes cannot be  
 268 called truly model-agnostic because some models do not require them, but neither are  
 269 they fully model-specific. To ensure maximum usability for different models, workflows  
 270 must be as modular as possible so that modelers can mix and match from available code  
 271 to suit the particularities of their chosen model (i.e., our third design principle, described  
 272 later).

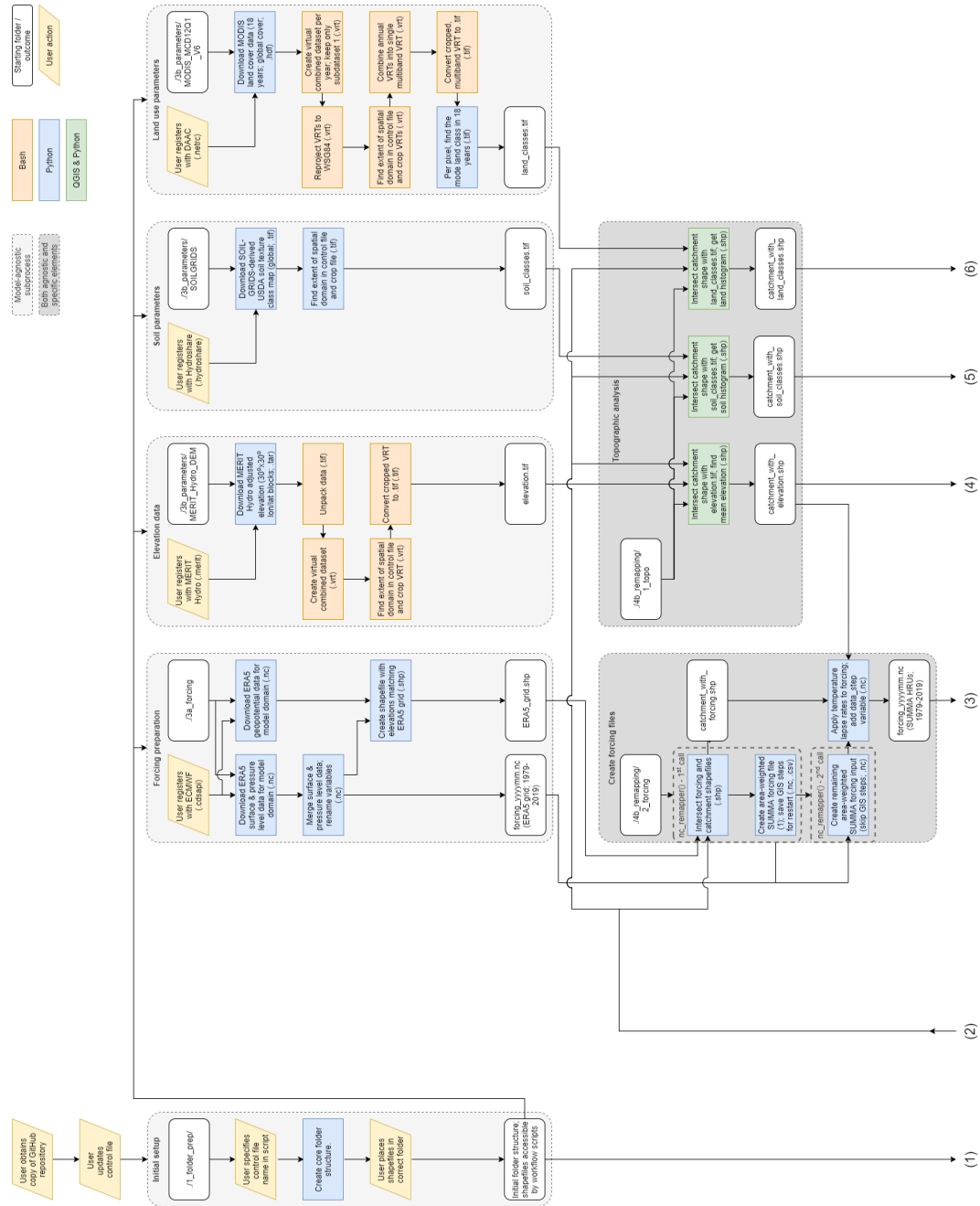


**Figure 3.** Model-agnostic configuration steps. Each rectangular block corresponds to a specific model setup task and is accompanied by a specific script with Python or Bash code, stored in a GitHub repository. Rounded rectangles indicate starting points of specific sub-tasks (mainly showing which folder in the repository contains certain parts of the workflow) and the outcomes of each sub-process. Parallelograms indicate actions the user must perform. Numbers show connections with the model-specific configuration tasks in Figure 4.

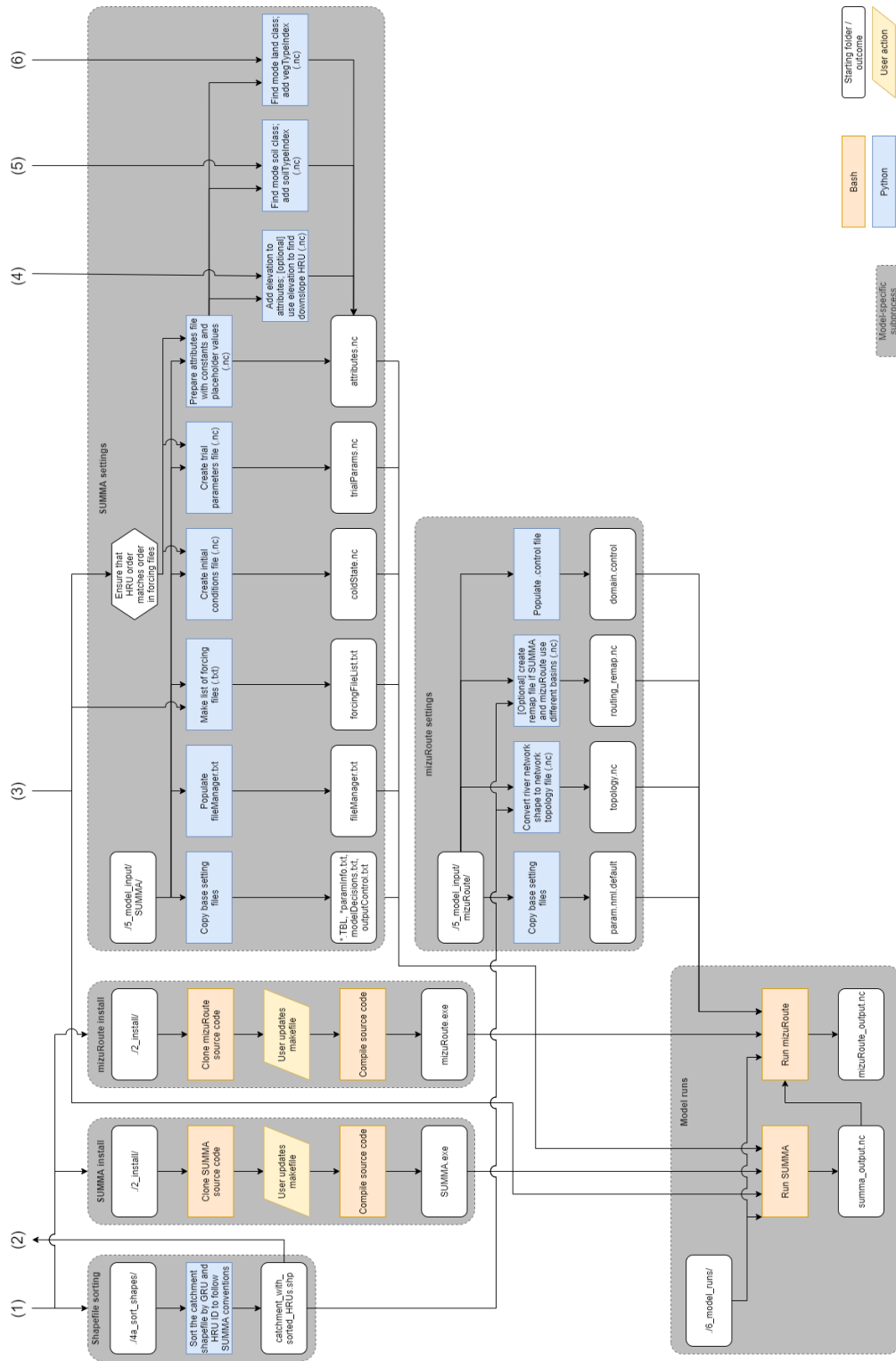


**Figure 4.** Model-specific configuration steps. Each rectangular block corresponds to a specific model setup task and is accompanied by a specific script with Python or Bash code, stored in a GitHub repository. Rounded rectangles indicate starting points of specific sub-tasks (mainly showing which folder in the repository contains certain parts of the workflow) and the outcomes of each sub-process. Parallelograms indicate actions the user must perform. The hexagon indicates an aspect of SUMMA’s input requirements (i.e., not an action or script) and is shown to clarify why creating the forcing files is on the critical path towards creating the other necessary model configuration files. Numbers show connections with the model-agnostic configuration tasks in Figure 3.

273

## 2.2 General layout and workflow control

274

275

276

277

278

279

280

281

282

283

Our second design principle prescribes an intuitive interface for hydrologic modelers. We recognize two elements here: first, the code and data structure must be clear and easy to understand. Second, interacting with the workflow must be straightforward. Our example implementation strives to achieve both of these goals through a clean separation of code and data and the use of a single configuration file (hereafter referred to as a “control file”) that outlines high-level workflow decisions such as file paths, spatial and temporal extent of the experiment, and details about the shapefiles that contain the domain discretization. Using configuration or control files is common practice in software design applications (see e.g. Sen Gupta et al., 2015) and avoids the need to introduce hardcoded elements such as file paths and variable values in the code itself.

284

285

286

287

288

289

290

291

In a typical application of our example workflow, the user first creates a local copy of the code provided on our GitHub repository. We refer to this local code as the “code directory”. The workflow is set up to store all data for a given modeling domain in a user-specified data folder (referred to as the “data directory”). This allows a clean separation between the workflow code itself and the data downloaded and preprocessed by the workflow code (Figure 5). The workflow’s default settings ensure that the data directory is populated with folders and subfolders with descriptive names, making navigation of the generated data clear.

292

293

294

295

296

297

298

299

300

301

302

303

304

305

306

307

308

309

310

Figure 6 shows part of the control file that defines the modeling domain for a model configuration for the Bow River at Banff, Canada (the full file is included as part of the repository; see Section 3 for a description of this test case). The control file contains the high-level information needed by the workflow, such as the name of the user’s shapefiles, the names of required attributes in each shapefile, the spatial extent of the modeling domain, the years for which forcing data should be downloaded, and file paths and names for all required data. The workflow scripts read information from the control file as needed. Keeping all information in one place enables a user to quickly generate model configurations for multiple domains, without needing to scour all individual scripts for hardcoded file paths, domain extents, etc. For example, changing the simulation period for a given domain requires changing two values in the control file, after which selected code can be re-run to download and preprocess the necessary forcing data and run new simulations. To configure our chosen models for a new domain (assuming that no changes to the model or desired data sets are introduced), a user only needs to provide a new domain discretization file and update in the control file the name of the domain (so that a new data folder can be generated), the names of the discretization files, and the bounding box of the new domain. The workflow can then be fully re-run to create a model configuration for the new domain, without any changes being made to the workflow scripts themselves.

311

## 2.3 Flexibility at each step of model setup

312

313

314

315

316

317

Our third design principle recognizes that process-based models are complex entities and that the setup procedures for any given model are model- or even experiment-specific. Not all models will need to go through the same configuration steps, nor will every model experiment need the settings as defined in our example workflow. Our example workflow (Figure 2-4; details in Appendix A) aims to encourage adaptation beyond our original application through modularity and extensive documentation.

318

319

320

321

322

323

First, we have chosen to present the workflow as a collection of scripts rather than a package or module so that the user has straightforward access to the workflow code. This presentation simplifies adapting the code to different models or experiments. Second, the workflow separates model setup into numerous small tasks (Figure 2-4) and saves all intermediate results to files. This modularity makes it straightforward to branch out from our chosen defaults at any given step in the modeling chain. Third, for this iter-

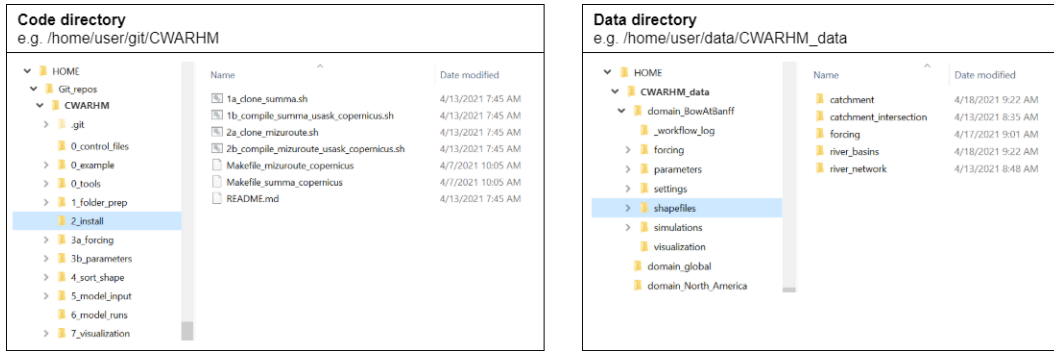


**Figure 5.** Example of separated code and data directories. The code directory (left) contains the same data and scripts as available on the repository’s GitHub page. The data directory (right) contains the shapefiles, forcing data, parameter data, setting files and model simulations.

```

# CWARHM-SUMMA workflow setting file.
# Characters '|' and '#' are used as separators to find the actual setting values. Any text behind '|' is assumed to be part of the setting value, unless preceded by '!'.
# Note on path specification
# If deviating from default paths, a full path must be specified. E.g. '/home/user/non-default/path'

# Modeling domain settings
root_path | /project/gwf/gwf_cmt/wknoben/CWARHM_data | # Root folder where data will be stored.
domain_name | BowAtBanff | # Used as part of the root folder name for the prepared data.

# Shapefile settings - SUMMA catchment file
catchment_shp_path | default | # If 'default', uses 'root_path/domain_name/shapefiles/catchment'.
catchment_shp_name | bow_distributed_elevation_zone.shp | # Name of the catchment shapefile. Requires extension '.shp'.
catchment_shp_gruid | GRU_ID | # Name of the GRU ID column (can be any numeric value, HRUs within a single GRU have the same GRU ID).
catchment_shp_hruid | HRU_ID | # Name of the HRU ID column (consecutive from 1 to total number of HRUs, must be unique).
catchment_shp_area | HRU_area | # Name of the catchment area column. Area must be in units [m^2].
catchment_shp_lat | center_lat | # Name of the latitude column. Should be a value representative for the HRU. Typically the centroid.
catchment_shp_lon | center_lon | # Name of the longitude column. Should be a value representative for the HRU. Typically the centroid.

# Shapefile settings - mizuRoute river network file
river_network_shp_path | default | # If 'default', uses 'root_path/domain_name/shapefiles/river_network'.
river_network_shp_name | bow_river_network_from_merit_hydro.shp | # Name of the river network shapefile. Requires extension '.shp'.
river_network_shp_segid | COMID | # Name of the segment ID column.
river_network_shp_downsegid | NextDownID | # Name of the downstream segment ID column.
river_network_shp_slope | slope | # Name of the slope column. Slope must be in units [length/length].
river_network_shp_length | length | # Name of the segment length column. Length must be in units [m].

# Shapefile settings - mizuRoute catchment file
river_basin_shp_path | default | # If 'default', uses 'root_path/domain_name/shapefiles/river_basins'.
river_basin_shp_name | bow_distributed.shp | # Name of the routing subbasins shapefile needed for remapping. Requires extension '.shp'.
river_basin_shp_rm_hruid | COMID | # Name of the routing basin ID column.
river_basin_shp_area | area | # Name of the catchment area column. Area must be in units [m^2].
river_basin_shp_hru_to_seg | hru_to_seg | # Name of the column that shows which river segment each HRU connects to.

# Shapefile settings - SUMMA-to-mizuRoute
river_basin_needs_remap | no | # 'no' if routing basins map 1:1 onto model GRUs. 'yes' if river segments span multiple GRUs or if multiple segments are inside a single GRU.

# Install settings
github_summa | https://github.com/CH-Earth/summa | # Replace this with the path to your own fork if you forked the repo.
github_mizuroute | https://github.com/ncaar/mizuroute | # Replace this with the path to your own fork if you forked the repo.
install_path_summa | default | # If 'default', clones source code into 'root_path/installs/summa'.
install_path_mizuroute | default | # If 'default', clones source code into 'root_path/installs/mizuRoute'.
exe_name_summa | summa.exe | # Name of the compiled executable.
exe_name_mizuroute | mizuroute.exe | # Name of the compiled executable.

# Forcing settings
forcing_raw_time | 2008,2013 | # Years to download: Jan-[from],Dec-[to].
forcing_raw_space | 51.74/-116.55/50.95/-115.52 | # Bounding box of the shapefile; lat_max/lon_min/lat_min/lon_max. Will be converted to ERA5 download coordinates
forcing_time_step_size | 3600 | # In script. Order and use of '/' to separate values is mandatory.
forcing_measurement_height | 3 | # Size of the forcing time step in [s]. Must be constant.
forcing_shape_path | default | # Reference height for forcing measurements [m].
forcing_shape_name | era5_grid.shp | # If 'default', uses 'root_path/domain_name/shapefiles/forcing'.
forcing_shape_lat_name | lat | # Name of the forcing shapefile. Requires extension '.shp'.
forcing_shape_lon_name | lon | # Name of the latitude field that contains the latitude of ERA5 data points.
forcing_geo_path | default | # Name of the longitude field that contains the longitude of ERA5 data points.
    
```

Setting	Value	Description
github_summa	https://github.com/CH-Earth/summa	Replace this with the path to your own fork if you forked the repo.
github_mizuroute	https://github.com/ncaar/mizuroute	Replace this with the path to your own fork if you forked the repo.
install_path_summa	default	If 'default', clones source code into 'root_path/installs/summa'.
install_path_mizuroute	default	If 'default', clones source code into 'root_path/installs/mizuRoute'.
exe_name_summa	summa.exe	Name of the compiled executable.
exe_name_mizuroute	mizuroute.exe	Name of the compiled executable.
forcing_raw_time	2008,2013	Years to download: Jan-[from],Dec-[to].
forcing_raw_space	51.74/-116.55/50.95/-115.52	Bounding box of the shapefile; lat_max/lon_min/lat_min/lon_max. Will be converted to ERA5 download coordinates
forcing_time_step_size	3600	In script. Order and use of '/' to separate values is mandatory.
forcing_measurement_height	3	Size of the forcing time step in [s]. Must be constant.
forcing_shape_path	default	Reference height for forcing measurements [m].
forcing_shape_name	era5_grid.shp	If 'default', uses 'root_path/domain_name/shapefiles/forcing'.
forcing_shape_lat_name	lat	Name of the forcing shapefile. Requires extension '.shp'.
forcing_shape_lon_name	lon	Name of the latitude field that contains the latitude of ERA5 data points.
forcing_geo_path	default	Name of the longitude field that contains the longitude of ERA5 data points.

**Figure 6.** Part of a workflow control file, showing settings for the Bow at Banff test case (test cases described in Section 3). The “Setting” column contains specific strings that each script in the repository looks for to identify which line in the control file contains the information the script needs. The “value” column contains the actual settings, such as file paths, shapefile identifiers, etc. Descriptions of each field are included for the user’s benefit but not used by the setup scripts.

324 ation of our workflow, we have chosen to move high-level decisions into the control file  
325 and leave various modeling decisions as assumptions in the workflow scripts. We have  
326 spent considerable effort on documenting any such assumptions (see Appendix A) to let  
327 advanced users make targeted changes to the workflow code. Examples of these decisions  
328 include the number of soil layers used across the modeling domain, values for the initial  
329 model states, and default routing parameters. In future versions of our workflow, such  
330 decisions may be moved to a dedicated experiment-control file.

## 331 2.4 Code provenance

332 Our fourth design principle relates to traceability. The decision to separate code  
333 and data directories potentially introduces a disconnect between code and data, and sit-  
334 uations may arise where it is no longer clear which version of a given piece of code gen-  
335 erated a particular piece of data. This can happen in cases where the workflow code is  
336 updated after having already been used to create (part of) a model configuration. Al-  
337 though the changes to the workflow code can be tracked through version control systems  
338 such as Git, it is much more difficult to trace which version of the code generated the  
339 data. Every script in our example workflow therefore places both a log file and a copy  
340 of its code in the data sub-directory on which it operates. This ensures that, even if a  
341 user makes changes to the code directory, a record exists in the data directory of the spe-  
342 cific code used to generate the files in that data directory. Copies of the model settings  
343 are stored in their simulation data directories by default so that simulation provenance  
344 can be traced as well.

## 345 3 Test cases

346 We have implemented a workflow for model configuration using the SUMMA and  
347 mizuRoute models. For brevity, details about both models and a detailed description of  
348 each step shown in Figure 2-4 can be found in Appendix A. This section briefly describes  
349 the two test cases that we used to test our workflow code.

### 350 3.1 Continental model instantiation

351 This first test case uses 40 years of forcing data to simulate hydrologic processes  
352 over the North American continent to illustrate the large-domain applicability of our ap-  
353 proach. The continental domain is divided into 517,315 sub-basins or Grouped Response  
354 Units (GRUs; median GRU size is 33 km<sup>2</sup>; mean size is 40 km<sup>2</sup>) derived from the global  
355 MERIT basins data set (Lin et al., 2019). Simulations are run from 1979-01-01 to 2019-  
356 12-31 at a 15-minute temporal resolution to facilitate numerical convergence of the model  
357 equations. Figure 7 shows summary statistics of several simulated variables: as expected,  
358 snow accumulation tends to be higher in mountainous and higher-latitude locations; to-  
359 tal soil water values are lower in the arid regions of the central and western US and Canada  
360 and northern Mexico; evapotranspiration rates fluctuate according to available energy  
361 (latitude) and water; and large river networks are clearly visible as a result of accumu-  
362 lation of upstream river flow. These results are outputs from a model run with default  
363 parameters and are unlikely to be accurate for any given location (see also a caution-  
364 ary note on the use of global data products in Appendix B). However, the visible large-  
365 scale patterns appear hydrologically sensible, giving us confidence that the initial model  
366 configuration is a solid basis for further model improvement and development. More im-  
367 portantly, the workflow documents every decision made during model configuration, en-  
368 abling repeatable simulations of this model domain with only a fraction of the original  
369 effort needed.

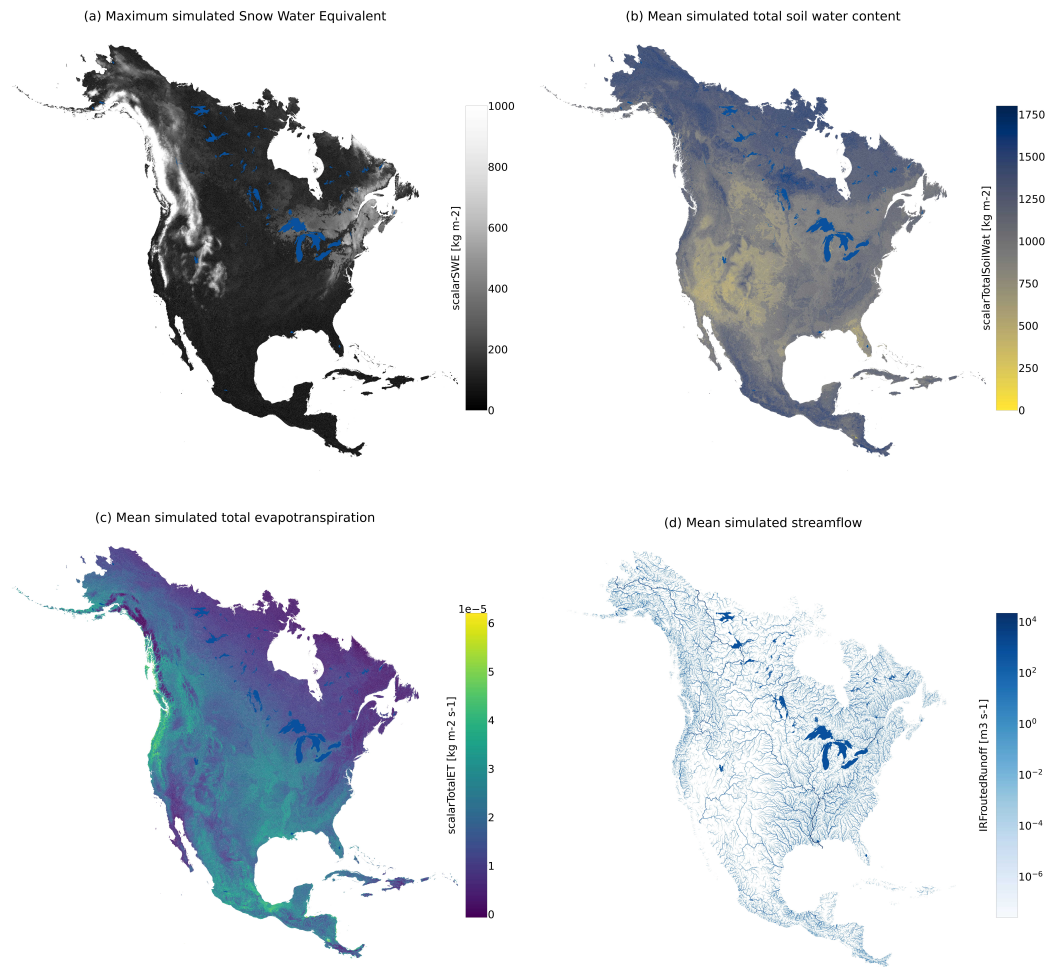


**Figure 7.** Overview of large-domain simulations. SUMMA does not simulate lake hydrology, and no calculations are performed for GRUs that are completely classified as open water. Lake delineations of lakes  $> 1,000 \text{ km}^2$  are obtained from the HydroLAKES data set (Messenger et al., 2016) and used to mask such open-water GRUs in this figure. Model setup uses default parameter values – results for illustrative purposes only. (a) Maximum simulated Snow Water Equivalent per GRU is capped at  $1000 \text{ [kg m}^{-2}\text{]}$  for visualization purposes. (b) Mean simulated total soil water content, which includes both liquid and solid water in the soil profile. (c) Mean simulated evapotranspiration, defined as the sum of evaporation from the soil profile and the canopy, and transpiration by vegetation. Positive values in this image indicate evapotranspiration, while negative values indicate condensation (note that this is the inverse of how evapotranspiration values are stored in the SUMMA output files). (d) Mean runoff as determined by mizuRoute's Impulse Routing Function approach.

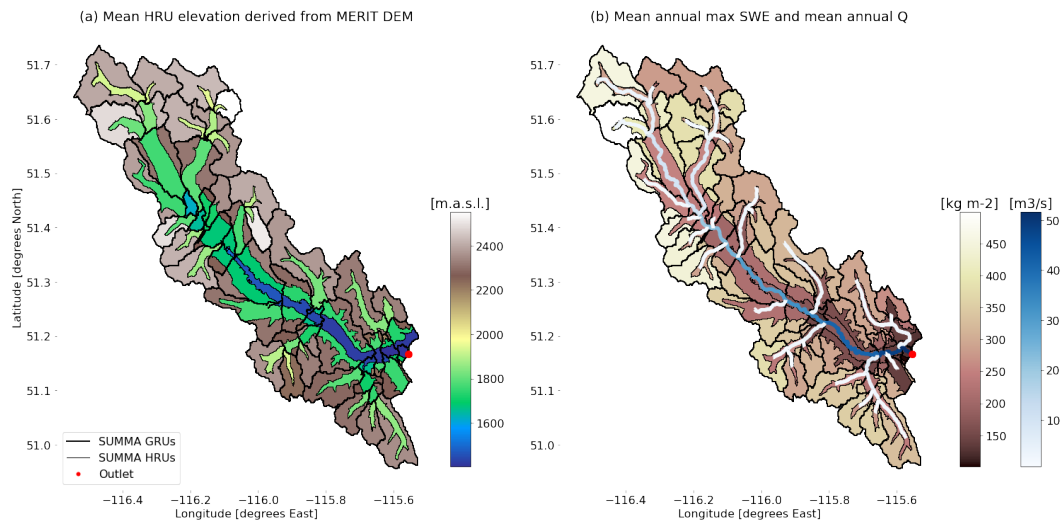


**Figure 8.** (a) Mean HRU elevation as derived from MERIT Hydro DEM. (b) Mean of maximum SWE per water year shown for each HRU, and mean annual streamflow shown for each river segment. Only data from complete water years is included. Model setup uses default parameter values – results for illustrative purposes only.

370

### 3.2 Local model instantiation

371

372

373

374

375

376

377

378

379

380

381

382

383

A SUMMA Grouped Response Unit (GRU) can be subdivided in as many Hydrologic Response Units (HRUs) as the modeler thinks practical and relevant and these HRUs can be used, for example, to represent different elevation zones, differences in soil or land use, differences in topography, or a combination of several of these elements. As a more localized test case, we created a subset of the MERIT basins data set (Lin et al., 2019) that covers the Bow River (Alberta, Canada) from its source in the Canadian Rocky Mountains to the town of Banff, Canada. We then sub-divided each MERIT sub-basin (GRUs in SUMMA terms) into multiple HRUs based on 500m elevation increments (Figure 8a), created a new control file for this new domain, and re-ran the workflow code. No changes were necessary to any of the workflow scripts because the scripts obtain all the required information from the updated control file and the code is generalized to handle both the large-domain case, where GRUs are not sub-divided into HRUs, and this local case, where HRUs are used.

384

385

386

387

388

389

390

391

392

393

394

395

396

397

398

This test case uses hourly forcing data from 01-01-2008 to 31-12-2013 (again run at a 15-minute sub-step resolution). Temperature lapse rates are applied to the forcing data for each individual HRU (see the “Create forcing files” box in Figure 3), meaning that the hydrometeorological conditions are somewhat different in each HRU despite the forcing grid cells being relatively large compared to the delineated catchments (see Figure 13). Figure 8b shows that simulated Snow Water Equivalent (SWE) varies per HRU and accumulated streamflow varies per stream segment. These figures provide a rudimentary test of the generated model setup (see also a cautionary note on the use of global data products in Appendix B). As may be expected, more snow accumulates at higher elevations, whereas the valley bottoms have a lower snowpack due to warmer air temperatures but larger flows due to their larger accumulated upstream area. As with the continental simulations, this local test case is fully reproducible and all model configuration decisions are stored as part of the workflow. This local test case also shows that different model configurations (in terms of spatial discretization in GRUs and HRUs) can be generated by the same model-specific workflow code.

## 4 Discussion

### 4.1 To what extent does our workflow fulfill reproducibility requirements?

Best practices for open and reusable computational science can be briefly summarized as follows (e.g. Gil et al., 2016; Hutton et al., 2016; Stodden and Miguez, 2013): data must be available and accessible, code and methods must be available and accessible, active development on issues with data, code, and methods must be possible, and licensing of data and code should be as permissive as possible. These requirements are formalized in the FAIR principles (Findable, Accessible, Interoperable, Reusable; Wilkinson et al., 2016) but by themselves are not enough to guarantee reproducibility of computational science (e.g., Añel, 2017; Bast, 2019; Hut et al., 2017). To be fully reproducible, details about hardware, software versions, and data versions also need to be recorded and shared (e.g. Choi et al., 2021; Chuah et al., 2020; Essawy et al., 2020). Such practices require a certain time investments but the benefits are clear: the resulting science is more transparent, can be more easily reproduced, and follow-up work can will be more efficient because less time is spent on mundane tasks such as data preparation.

Sandve et al. (2013) outline ten rules for reproducible computational science in the field of Computational Biology, and these are also applicable to Earth System modeling. Our workflow follows nine of these guiding principles:

- (1) Our workflow stores copies of the scripts that generate data together with the data itself, which allows a researcher to track how a given result was produced;
- (2) Our workflow contains no manual data manipulation: all changes to the data are done in scripts and can be traced;
- (3) An exact version of all software used is tracked, partly as installable Python environments and partly on the workflow repository for command line utilities;
- (4) All scripts are version controlled on the GitHub repository;
- (5) Our workflow is highly modular and stores intermediate results in individual folders to aid in debugging of setups and to allow easy diversion from our workflow;
- (6) All data that may support analysis and figures are systematically stored in a logical folder structure;
- (7) Our chosen model structure is flexible in prescribing outputs, removing a need to modify the model source code to display specific results;
- (8) Our visualization code keeps a precise record of which results file contains the data that underpin a given figure and thus a record exists of which data support a given textual statement about the analysis;
- (9) The workflow code is publicly accessible.

Their tenth principle, keeping accurate note of the seeds that underpin any element of randomness in the analysis, does not apply here. Sandve et al. (2013) also recommend sharing access to simulation results. This can be done through repositories such as HydroShare or Pangaea but may be infeasible in the case of large-domain Earth System modeling. For example, storing all input and output data of our continental test case would take approximately 13 TB.

Internal tests on different hardware and by different researchers indicate that our workflow effectively implemented these principles in practice: the workflow can be used to generate identical model inputs and outputs by specifying exact library, package, and model versions. Some caveats apply, however. Although it is possible to trace model source code versions through Git commit IDs, such IDs can obviously not account for local code modifications that are not tracked through Git and good “lab hygiene” is needed to ensure consistency between what is reported to have been done and what has in fact been done. Further, not all data sets that underlie our model setups have Digital Object Identifiers assigned to specific versions of the dataset. Given the size of the data sets involved,

449 sharing the data itself is infeasible, and some care must be taken to precisely track when  
450 data were downloaded as a means of making the use of data without DOIs traceable. Last,  
451 reproducibility is ensured through specifying exact versions of packages and libraries but  
452 many of these packages and libraries are undergoing rapid development and new versions  
453 are released constantly. There is a potential issue for reproducibility if older software ver-  
454 sions for one reason or another are no longer available (though for fully open-source soft-  
455 ware this should theoretically not happen). New versions of specific software may how-  
456 ever become incorporated into a new version of a workflow if they provide some needed  
457 functionality. To ensure backward compatibility, such new workflow versions must there-  
458 fore also be assigned a new DOI so that any specific workflow version can be tracked and  
459 re-used when needed.

## 460 **4.2 Towards community modeling**

### 461 *4.2.1 Short-term benefits of using workflows*

462 This paper introduces a modular model configuration workflow that separates model-  
463 agnostic and model-specific configuration steps. The two main benefits of approaching  
464 environmental modeling from this angle are clear: configuring multiple modeling exper-  
465 iments becomes much more efficient, and results are reproducible, because all model con-  
466 figuration decisions can be traced. These benefits address two problems that currently  
467 affect Earth System modeling. First, creating a typical model configuration is both dif-  
468 ficult and time consuming, and it is possible that model configuration tasks do not re-  
469 ceive the attention they deserve. Code may not be checked as thoroughly as may be nec-  
470 essary because bugs may not be readily apparent, and any time spent on model config-  
471 uration is consequently not spent on writing journal articles or meeting report deadlines.  
472 Configuring models can be more efficient if model configuration code is freely and openly  
473 shared. This enables time that is currently spent on creating model configurations to in-  
474 stead be spent on in-depth analysis, improving the model representation of real-world  
475 processes, and fixing any bugs that may be found in the configuration code or the model  
476 source code. If bugs are found, tracing the experiments that are affected by these bugs  
477 is possible, and it will be clear which studies need to be corrected. Openly shared model  
478 configuration code therefore has the potential to increase the robustness of model sim-  
479 ulations and accelerate advances in modeling capabilities. Second, by publishing work-  
480 flow code alongside a manuscript, the provenance of scientific results remains traceable  
481 (see e.g., Hutton et al., 2016; Melsen et al., 2017). This can increase confidence in model  
482 results. It also enables more effective follow-up studies because all decisions that under-  
483 pin the original study can be found in the public domain.

### 484 *4.2.2 Long-term vision for community workflows*

485 We see workflows such as the one presented in this paper as the first step towards  
486 a community-wide modeling framework. Figure 9 illustrates an example of such a frame-  
487 work using the workflow code presented in this paper as examples of each framework layer  
488 (see also Miles, 2014; pp 57-58). In addition to a division between model-specific and model-  
489 agnostic tasks, we envision a framework that distinguishes between data-specific and data-  
490 agnostic preprocessing steps. Processing layers would be separated by standardization  
491 layers that prescribe the output format for the preceding processing layer and consequently  
492 the input format for the following processing layer. Community-wide agreement on the  
493 formats used in standardization layers will promote efficient interoperability of different  
494 data-specific processing modules, possibly as part of broader work on international hy-  
495 drologic standards (see e.g. HY\_Features; Blodgett and Dornblut, 2018). Using our work-  
496 flow as an example, we have created data-specific processing modules for ERA5 mete-  
497 orological data, SOILGRIDS-derived soil classes, MODIS-derived land classes, and a MERIT  
498 Hydro-derived DEM. These modules generate data in standardized formats (in this case,  
499 netCDF4 forcing data and GeoTIFF spatial maps) that in turn feed into the data-agnostic

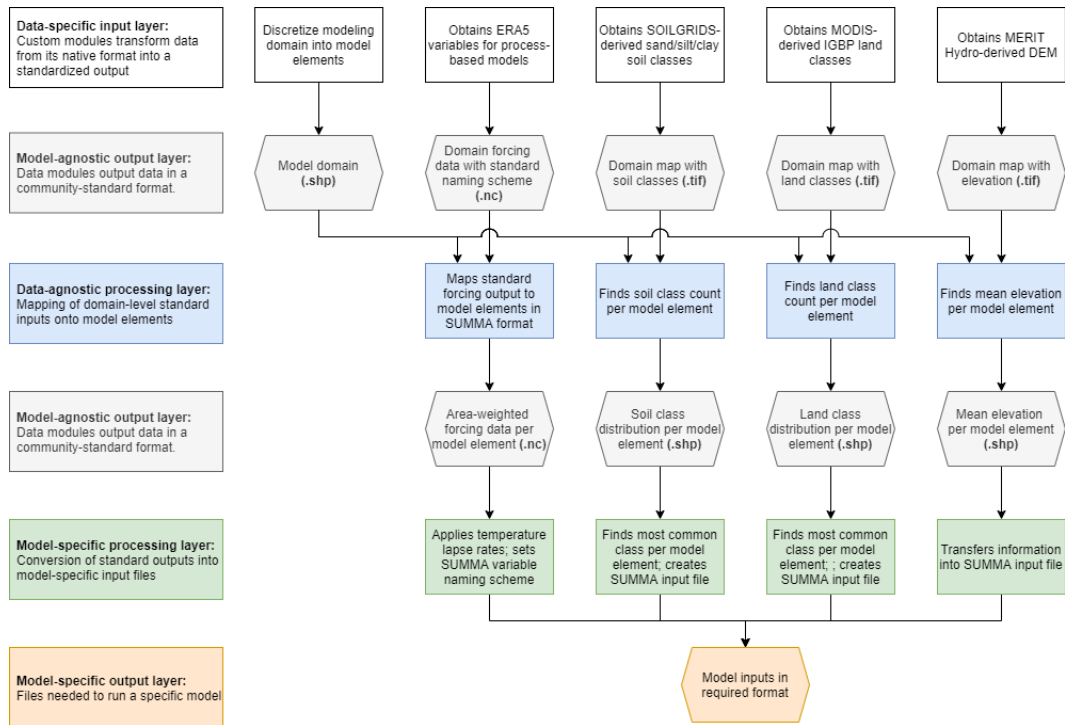


**Figure 9.** Schematic overview of a generalized community modeling framework, populated with examples from our SUMMA setup configuration workflow. Key to this modular approach is community-wide agreement on the formats used in each model-agnostic standardization layer. Such standards enable a modular approach to model-configuration, where existing modules can be seamlessly replaced, as long as they are designed to read and output data in the agreed-upon formats.

500 remapping layer. This layer generates further model-agnostic data in netCDF4 and Shapefile formats that are then transformed into SUMMA’s inputs through a model-specific  
 501  
 502 processing layer.

503 Our currently defined model-agnostic tasks are of course still implicitly SUMMA-  
 504 centric (i.e., we have completed those tasks because they generate the data that SUMMA  
 505 requires), though in principle the outputs can be immediately used by other models. The  
 506 modular nature of our workflow makes adding new datasets and processing steps as straight-  
 507 forward as writing new data-specific and data-agnostic routines and inserting them in  
 508 a further unchanged workflow. Changing to a different model requires writing a new model-  
 509 specific interface layer, but existing data processing scripts can remain untouched (again,  
 510 assuming that the new model has data needs that can be met by already existing data  
 511 modules). This means that the workflow can be tailored to a specific model or exper-  
 512 iment in a fraction of the time needed to create the model setup from scratch. The mod-  
 513 ified workflow can then be published alongside the new modeling results to keep those  
 514 results traceable.

515 It is of course possible that our attempt to separate model tasks is not equally ap-  
 516 plicable to every different model that is currently in use. In such cases, we hope that pro-  
 517 viding a tangible example of how the model configuration code can be organized and shared  
 518 in a structured way will nevertheless inspire others to create their own workflows. Mod-  
 519 ifying our workflow or adapting it for different purposes in such ways is the second step  
 520 we anticipate as needed to move towards a community modeling paradigm. By creat-

ing new or modifying existing workflows for new experiments and models, the required structure of a generalized model setup workflow may become apparent. As a third and final step, this generalized workflow can be formalized into a community-driven modeling framework that enhances efficiency and transparency in Earth System modeling.

To initiate the process of creating a community-driven modeling framework, our workflow is available as open-source code: <https://github.com/CH-Earth/CWARHM> (last access: 2021-12-03). We have chosen a permissive license that allows others to freely use and modify our code under the conditions that the modified code base is published under the same license, with attribution of its source and a list of changes. We envision a gradual process in which our repository is modified by others (either piecemeal or by incorporating our entire codebase in a new repository as, for example, a Git submodule), increasingly more data-specific and models-specific processing capabilities are made public, and appropriate formats for standard file formats become apparent. Deciding if and how to integrate these different elements into a single modeling framework is a decision the community will need to make in due course.

#### 4.2.3 *Where do workflows stand in the existing reproducibility landscape in hydrologic modeling?*

We approach the workflow problem from a catchment modeling perspective within the wider Earth System modeling community (see the definitions of different communities in Archfield et al., 2015). Calls for more efficient, transparent, and shareable model configuration approaches are not new in the catchment modeling community (see e.g., Blair et al., 2019; Famiglietti, et al., 2011; Hutton et al., 2016; Tarboton et al., 2009; Weiler and Beven, 2015) and considerable progress along these lines has been made. For example, Sen Gupta et al. (2015) standardize model inputs and outputs to efficiently couple a snow accumulation and melt routine with an existing open source modeling framework; Miles and Band (2015) develop a Python API that automatically preprocesses ecohydrologic parameter fields and forms the basis of a model configuration workflow for the RHESSys model (Miles, 2014); the Landlab toolkit (Bandaragoda et al., 2019) provides a general interface for building and coupling multiple models; Gan et al. (2020) integrate a web-based hydrologic model service with a data sharing system to promote reproducible workflows; HydroDS (Gichamo et al., 2020) is a web-based service that can be used to prepare input data for modeling; Bennett et al. (2020) create a tool to estimate hourly forcing input for physics-based models from commonly available daily data; Bavay et al. (published online 2020; under review) describe a tool that can be used to effectively create a Graphical User Interface for a given model; Essawy et al. (2020) provide an example of how containerization (storing a full computational environment into a software container) enhances reproducibility; and Kurtzer et al. (2017) develop a means of saving and transferring software and computing environments on and between High Performance Computing clusters. Put together, most if not all elements for fully reproducible, easy-to-use, computational hydrology already exist. So far however, uptake of these tools is regrettably not widespread.

We speculate that uptake of existing tools is somewhat low for multiple reasons. First, these tools are typically provided as self-contained packages. Packages tend to be easy to use for their intended purpose but take time to understand and do not necessarily provide much flexibility to deviate from their intended purpose. Layering additional functions on top of an existing package or modifying a package’s source code is certainly possible, but can be outside the comfort zone of many users. Second, several of these tools are provided as web-based services. This can be appealing because, for example, data can be pre-downloaded to speed up model configuration and model simulations can be easily shared. The advantage of such approaches is that they can be combined with some form of server-side data transformations (e.g., subsetting or averaging), which minimizes data transfers. Storing the inputs for and outputs of large-domain simulations can, how-

573 ever, be cumbersome, and keeping pre-downloaded data up-to-date and sufficient for all  
574 user needs takes sustained, long-term effort. A further complication is that it is regret-  
575 tably common that such web-based services require some form of manual interaction with  
576 the webpage, limiting opportunities to automate data acquisition tasks. Third, the lack  
577 of community agreement on standard data formats means that developers of new tools  
578 typically decide to have their tool output data in a format relevant to their own appli-  
579 cation, which may not be a format that is widely used by others. It is cumbersome for  
580 developers to have their tools ingest multiple different data formats and such function-  
581 ality is therefore somewhat rare. Community-wide agreement on a set of standard data  
582 formats, such as proposed in Figure 9, will make it easier for developers to know which  
583 data formats their tools must be able to ingest and produce to guarantee seamless in-  
584 teraction with other existing tools.

585 In short, some of the existing tools may be overdesigned or unsuitable for where  
586 the majority of the community currently stands. Such tools are typically designed by  
587 a small group of people, using a proof of concept or test case that is directly applicable  
588 to the developers' own work. Developers can make educated guesses about how their tool  
589 can be made more general beyond their proof of concept, but actually doing so typically  
590 relies on the original developers having both the motivation and opportunity to imple-  
591 ment functionality for others (e.g., incorporating new data sets or including model-specific  
592 layers for other models) or on new developers being willing to first understand the ex-  
593 isting package or web-service and then modifying it.

594 Our approach to provide a tangible example of how to structure model configura-  
595 tion tasks is different. First, our use of scripts instead of packages is likely much more  
596 similar to how many models are currently configured, which makes the barrier to try-  
597 ing our approach low. Second, our use of standardization layers that require interme-  
598 diate files to be in commonly used data formats makes it easy to adapt small parts of  
599 our workflow without needing to change any upstream or downstream configuration tasks.  
600 Third, there are clear and immediate benefits of adopting a workflow approach of the  
601 type proposed in this paper that are unrelated to how widely (or not) this approach is  
602 adopted: creating new configurations for the models used in such workflows will be more  
603 efficient and the resulting science will stand on a firmer foundation than closed-source  
604 results. Should our approach become more widely adopted then the path to a commu-  
605 nity modeling framework builds itself: as more examples of model configuration work-  
606 flows become available, our preliminary sketch of a community modeling framework in  
607 Figure 9 can be refined or redrawn. How to design, build, and maintain such a commu-  
608 nity framework can be decided in due course, and appropriate funding may be sought  
609 when needed, instead of preemptively securing funding to build modeling infrastructure  
610 without knowing how high community uptake of such infrastructure will be or which func-  
611 tionality the community is looking for. Advancing the paradigm of community model-  
612 ing requires active participation of the community. By providing an example of the first  
613 step in the process of designing the structure of a community modeling framework, we  
614 hope to encourage others to be part of this initiative.

## 615 5 Conclusions

616 This paper describes a code base that provides a general and extensible solution  
617 to configure hydrologic models. Specifically, the paper provides a tool that can be used  
618 to create reproducible configurations of the Structure for Unifying Multiple Modeling  
619 Alternatives (SUMMA, a process-based hydrologic model) and mizuRoute (a vector-based  
620 routing model). We consider this the implementation of a single model in a general frame-  
621 work that separates model-agnostic and model-specific configuration tasks. Such a sep-  
622 aration of tasks makes inclusion of new models in this framework relatively straightfor-  
623 ward because most of the data pre-processing code can remain unchanged and only model-  
624 specific code for the new model needs to be added.

625 The critical component of this framework is what we refer to as “standardization  
 626 layers”, which prescribe the details of the file formats that must come out of the preced-  
 627 ing processing layer and form the input of the following processing layer. By standard-  
 628 izing inputs and outputs, the code that forms the processing layers only needs to con-  
 629 cern itself with these prescribed formats. Changing specific processing modules to, for  
 630 example, pre-process a different data set, perform a different way of mapping data onto  
 631 model elements, or prepare input files for a different model, can therefore happen in iso-  
 632 lation from the remainder of the workflow as long as the new processing code accepts  
 633 and returns data in the prescribed formats. We show examples of this approach with multi-  
 634 decadal continental SUMMA and mizuRoute simulations, and with a local SUMMA con-  
 635 figuration that uses a more complex spatial discretization than the continental simula-  
 636 tions use.

637 Future work will involve adding model-specific code for multiple additional mod-  
 638 els and any needed data-specific preprocessing modules. We have termed this initiative  
 639 “Community Workflows to Advance Reproducibility in Hydrologic Modeling” (CWARHM;  
 640 “swarm”) and we encourage others to be part of this model-agnostic workflow initiative.  
 641 The configuration code for the SUMMA and mizuRoute setup shown in this manuscript  
 642 is available on GitHub: <https://github.com/CH-Earth/CWARHM> (last access: 2021-12-  
 643 03).

## 644 **Appendix A Workflow description**

645 This section describes in detail our example of a model setup workflow that follows  
 646 the design principles outlined in Section 2. The workflow code, model code, software re-  
 647 quirements, and data are fully open-source to follow the FAIR principles. The workflow  
 648 is written in Python and Bash, using input data with global coverage, a spatially dis-  
 649 tributed, physics-based hydrologic modeling framework designed to isolate individual mod-  
 650 eling decisions (Clark et al., 2015a, 2015b, 2021c), and a network routing model (Mizukami  
 651 et al., 2021, 2016) that connects the individual hydrologic model elements through a river  
 652 network. This example workflow can be used to generate a basic SUMMA and mizuRoute  
 653 setup anywhere on the globe and is designed such that the model-agnostic parts of the  
 654 code can easily feed into other modeling chains.

655 Part of the code in this repository is adapted from or inspired by work performed  
 656 at the National Centre for Atmospheric Research and the University of Washington.

### 657 **A1 Models**

658 This section provides a brief overview of SUMMA (Clark et al., 2015a, 2015b, 2021c)  
 659 and mizuRoute (Mizukami et al., 2021, 2016) to the extent relevant to understand our  
 660 workflow. We refer the reader to the original papers that describe each model for fur-  
 661 ther details. We selected both models for their flexible nature, computational capacity  
 662 to model very large domains, and availability of local expertise. Both models are writ-  
 663 ten in Fortran, and their source code needs to be compiled before the models can be used.

#### 664 ***A11 Structure for Unifying Multiple Modeling Alternatives (SUMMA)***

665 SUMMA is a process-based modeling framework designed to isolate specific mod-  
 666 eling decisions and evaluate competing alternatives for each decision, with the ability to  
 667 do so across multiple spatial and temporal configurations. SUMMA solves a general set  
 668 of mass and energy conservation equations (Clark et al., 2015a, 2021c) and includes mul-  
 669 tiple alternative flux parametrizations (Clark et al., 2015b). It separates the equations  
 670 that describe the model physics from the numerical methods used to solve these equa-  
 671 tions, allowing the use of state-of-the-art numerical solving techniques (Clark et al., 2021c).

SUMMA is available as Free and Open Source Software (FOSS) and under active development (see <https://www.github.com/CH-Earth/summa>).

SUMMA organizes model elements into Grouped Response Units (GRUs) that can each be further subdivided into multiple Hydrologic Response Units (HRUs). This enables flexible spatial discretization of modeling domains. For example, point-scale studies are possible by defining the domain as a single GRU that contains exactly one HRU (see e.g., Clark et al., 2015b; GRU area can be an arbitrary value because all fluxes and states are calculated per unit area). It is equally possible to mimic grid-based model setups such as commonly used in land-surface modeling schemes by defining each GRU to be equivalent to a grid cell and optionally using the HRUs to account for sub-grid variability (e.g., mimicking the tiled grid approach of traditional VIC and MESH setups; Liang et al., 1994; Pietroniro et al., 2007). Finally, GRUs can represent the (sub-)catchments of a given river system with HRUs being areas of similar hydrologic behavior within each GRU. Such model configurations can use GRUs and HRUs of irregular shape, which has several advantages over grid-based setups (see e.g., Gharari et al., 2020). Most importantly, such spatial configurations can accurately follow the actual topography of the modeling domain, and this makes model results easier to visualize and interpret. SUMMA is configured with irregularly shaped computational elements in the test cases presented in this paper.

### ***A12 mizuRoute***

mizuRoute is a vector-based river routing model specifically designed for large-domain applications such as modeling of hydrologic processes across a continental domain. It organizes the routing domain into Hydrologic Response Units (HRUs; i.e., catchments) and stream segments that meander through the HRUs and provide connections between them (Mizukami et al., 2021, 2016). It can process inputs from hydrologic models with both grid- and vector-based setups and provides different options for channel routing: Kinematic Wave Tracking (KWT) and Impulse Response Function (IRF). For a given stream segment, the IRF method constructs a set of unique Unit Hydrographs (UH) for each upstream segment which is used to route runoff from each upstream reach independently. In other words, the routed runoff in a given stream segment is a simple sum of the UH runoff generated in all upstream segments. The KWT method instead tracks channel runoff as kinematic waves moving through the stream network with their own celerity. mizuRoute is available as FOSS and under active development (see <https://github.com/ESCOMP/mizuRoute>).

### ***A13 Note on definitions***

SUMMA distinguishes between Grouped Response Units (GRUs) and Hydrological Response Units (HRUs). SUMMA's main modeling element is the GRU, which can be sub-divided into an arbitrary number of HRUs. SUMMA can handle GRUs and HRUs of any shape (e.g. points, grid cells, catchments) and these terms therefore refer to model elements of arbitrary shape and size. In this workflow, we use mizuRoute to route runoff between SUMMA's GRUs. Somewhat confusingly, mizuRoute refers to all routing basins as HRUs only and does not use the term GRU. As a result, what SUMMA calls GRUs are referred to as HRUs by mizuRoute. For consistency with both sets of documentation, we use their own terminology for model elements where possible. Figure 8 shows a graphical example of the differences in terminology.

## **A2 Workflow description**

This section briefly describes each step shown in the workflow diagram (Figure 2 in the main manuscript). Figures are generated using the test case configured for the Bow River catchment located in Alberta, Canada (see Figure 8 for an overview of this domain).

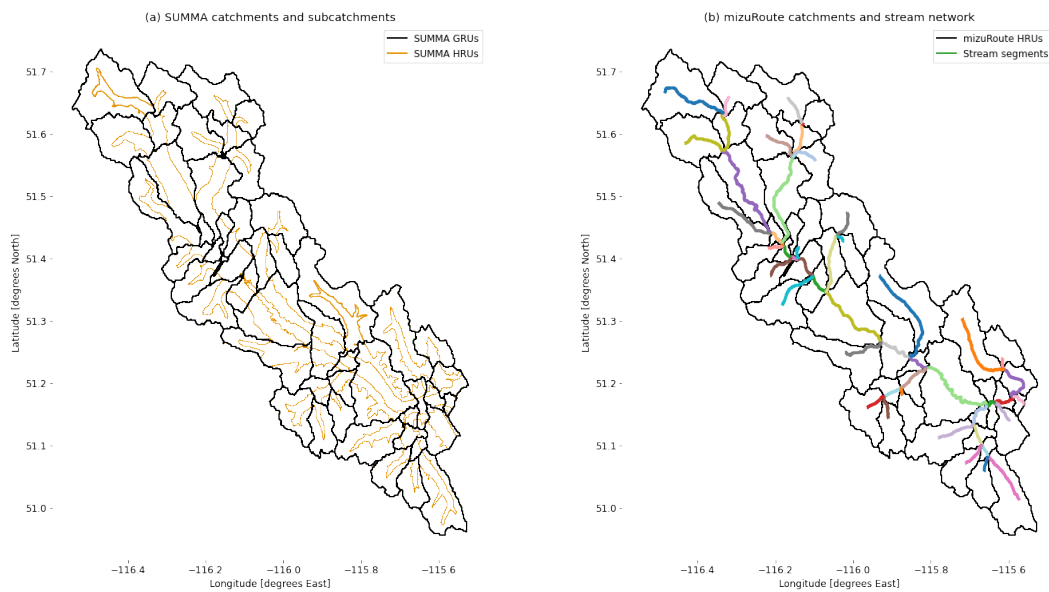


**Figure A1.** Catchment of the Bow River at Banff (Alberta, Canada) discretized into (a) SUMMA and (b) mizuRoute model elements, showing associated terminology. SUMMA HRUs in (a) represent different elevation bands within each SUMMA GRU. A SUMMA GRU always contains at least one SUMMA HRU. There is no upper limit to the number of HRUs a single SUMMA GRU can be divided into. A single SUMMA HRU is never part of more than one SUMMA GRU. In our example, SUMMA GRUs are identical to mizuRoute HRUs. mizuRoute stream segments are shown in different colors to emphasize that in this case each mizuRoute HRU maps 1:1 onto a single stream segment.

This test case covers a geographically small area (approximately 2200 km<sup>2</sup>) and uses a more complex model setup (SUMMA GRUs subdivided into multiple HRUs) than the continental test case (where SUMMA GRUs contain exactly one HRU each), making it the best choice to visualize model setup procedures. Italicized phrases in this section indicate folders, scripts, or variables as found in the GitHub repository. To start, a user would download or clone the complete GitHub repository. The following sections provide more detail about the scripts found within the GitHub repository. A summary of this section and a direct mapping of repository directories onto manuscript sections can be found in the Supporting Information. Although our workflow requires only limited user interaction to generate a model configuration for a new domain, we do make certain assumptions about this model configuration which users should be aware. These assumptions are specified in each subsection.

### A21 Workflow setup and folder structure

This section describes the steps “User updates control file” and the steps contained in the box “Initial setup” (Figure 2).

*A21.1 Control files* Control files are the main way for a user to interact with the workflow. They contain high-level information such as file paths, file names, variable names, and specification of the spatial and temporal extent of the modeling domain (see also Sen Gupta et al., 2015). A new control file needs to be created by the user for each new domain. As an example, the control file for the *Bow.at.Banff* test case is included as part of the Github repository, in the folder *./CWARHM/0\_control\_files*. The READMEs of each sub-folder on the GitHub repository contain a list of the settings in the control file on which the scripts in that sub-folder rely.

*A21.2 Folder preparation* The workflow separates generated data from the code used to generate the data. The script in the folder *./CWARHM/1\_folder\_prep* generates a basic data folder structure in a location of the user’s choosing (see Figure 3b). This basic folder structure generates a main data folder with a subdirectory for the current domain. In this domain folder, it further generates a dedicated folder where the user can place their shapefiles that delineate the SUMMA catchments (hydrologic model GRUs and HRUs), mizuRoute catchments (routing model HRUs), and mizuRoute river network. This is the only script in the workflow that needs to be manually modified if a setup for a new domain is generated. A user will need to modify the variable *sourceFile* so that it points to the control file for the current domain. In our example, this is set to *control\_Bow.at.Banff.txt*. The script then copies the contents of this control file into a new file called *control\_active.txt*, which is the file every other workflow script will search for. The variable *sourceFile* needs to be updated when a control file for a new domain is used. Note that the contents of the file *control\_active.txt* determine which folders and files the other workflow scripts operate on.

*A21.3 Domain shapefiles* With a basic folder structure in place, the user can now move their prepared shapefiles into the newly generated folders (assuming the control file uses ‘default’ values for these shapefile paths). Briefly, the shapefiles should contain: geometries that delineate the hydrologic model GRUs and HRUs, the routing model HRUs, and the routing model river network in a regular latitude/longitude projection (in other words, in the Coordinate Reference System defined by EPSG:4326; <https://epsg.io/4326> [last access, 2021-10-11]). Each shapefile needs to specify certain properties of the model domain, such as identifiers for each GRU, HRU, and stream segment; HRU area and centroid location, stream segment slope and length; and the stream segment ID into which a given HRU drains.

Detailed requirements for the shapefiles are provided in the README in `./CWARHM/1_folder_prep`. Example shapefiles for the *Bow.at.Banff* test case are part of the repository and can be found in the subfolders of `./CWARHM/0_example`.

## A22 Model-agnostic workflow elements

This section provides details about the model-agnostic elements of the workflow (shown in light grey in Figure 2). For convenience, this section is organized to follow the four model-agnostic sub processes: pre-processing of forcing, elevation, soil, and land use data.

*A22.1 Pre-processing of forcing data* Our chosen forcing product is the ERA5 reanalysis data set (Copernicus Climate Change Service (C3S), 2017; Hersbach et al., 2020) provided by the European Centre for Medium-Range Weather Forecasts (ECMWF). ERA5 data are available as hourly data for the period 1979 to present minus 5 days, at a 31 km spatial grid that covers the Earth’s surface or at a re-gridded  $0.25^\circ \times 0.25^\circ$  latitude/longitude resolution. ERA5 data preparation includes two-way interactions between atmosphere, land surface and ocean surface components. The ERA5 model setup includes different atmospheric layers and ERA5 data are available at 137 different pressure levels (i.e., heights above the surface), as well as at the surface. The lowest atmospheric level is L137, at geopotential and geometric altitude 10 m (i.e., 10 m above the land surface). To limit the influence of ECMWF’s land model on our required forcing variables (simulating the land surface response is SUMMA’s role after all), we obtain air temperature, wind speed, and specific humidity at the lowest pressure level (L137; Hersbach et al., 2017) instead of at the land surface. Precipitation, downward shortwave radiation, downward longwave radiation, and air pressure are unaffected by the land model coupling and can be downloaded at the surface level (Hersbach et al., 2018).

Surface and pressure level data are stored in two different data archives and are accessed in different ways. Download scripts for each separate archive are found in folder `./CWARHM/3a_forcing/1a_download_forcing`. These scripts access the C3S Climate Data Store (CDS) using the user’s credentials (instructions on how to obtain and store credentials can be found in the README in the download folder) and download the necessary data in monthly blocks of hourly data at a regular  $0.25 \times 0.25^\circ$  latitude/longitude resolution. The spatial and temporal extents of the domain are taken from the control file. As per the ERA5 documentation, ERA5 data should be seen as point data, even though standard visualization approaches typically show this kind of data as an interpolated grid. In our example workflow, we make the simple assumption that each ERA5 point contains forcing data that are representative for the grid of size  $0.25^\circ \times 0.25^\circ$  of which the grid point is the centroid. The workflow code automatically finds which ERA5 grid points to download based on the catchment bounding box specified in the control file (Figure 9). Once downloaded, the code in `./CWARHM/3a_forcing/2_merge_forcing` can be used to merge the surface and pressure level downloads into a single netCDF file, which is used for further processing. During this merging process, the ERA5 variable names are also changed to more descriptive ones.

Gridded forcing data does not map directly onto irregular model elements such as HRUs. Code in `./CWARHM/3a_forcing/3_create_shapefile` generates a shapefile for the forcing data that outlines the forcing grid (dotted red lines in Figure 9), which is later used to find the relative contribution of each forcing grid cell to the forcing of each HRU. The elevation of each ERA5 grid point is added to this shapefile. This information is later used to apply temperature lapse rates based on the difference in elevation of the ERA5 data and mean HRU elevations. As per the ERA5 documentation, the elevation of each ERA5 data point is found by dividing the geopotential [ $\text{m}^2 \text{s}^{-2}$ ] of each point (downloaded through scripts in `./CWARHM/3a_forcing/1b_download_geopotential`) by the gravitational acceleration [ $\text{m s}^{-2}$ ].

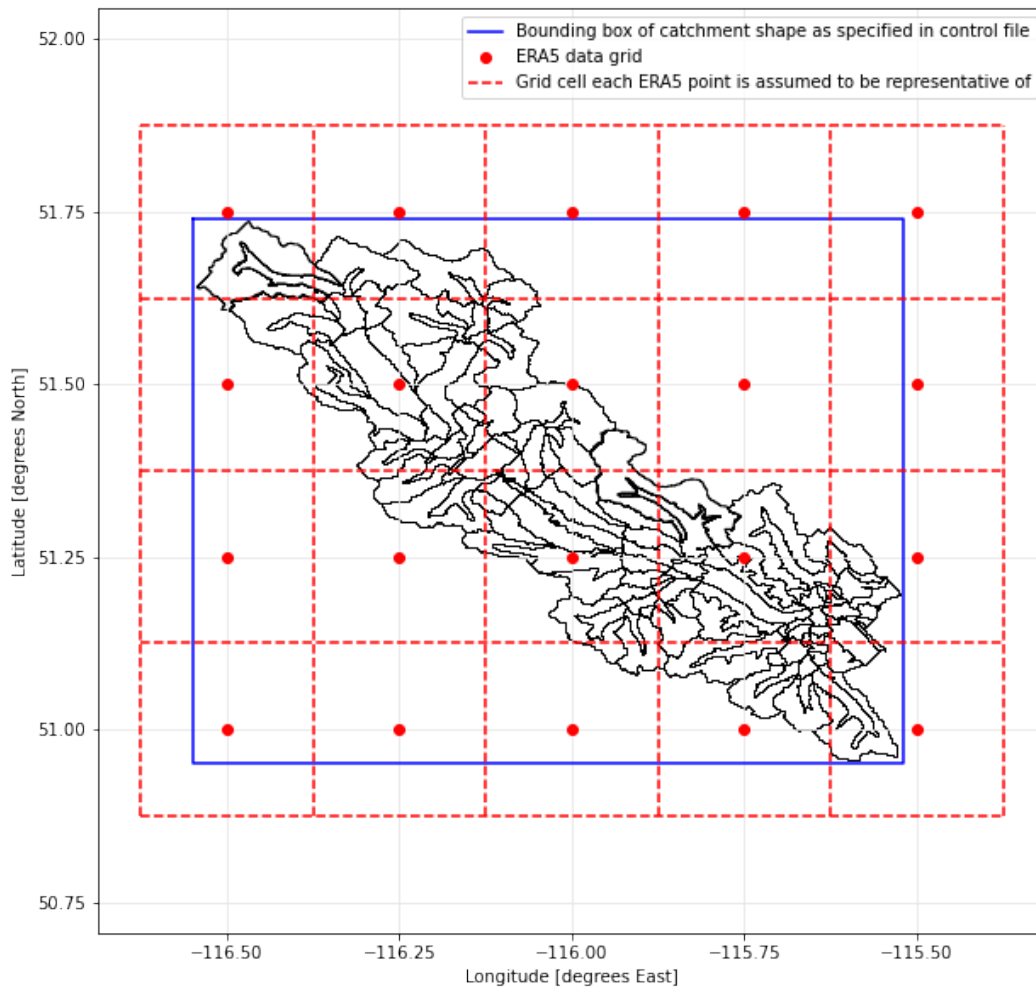


**Figure A2.** Overview of ERA5 data points, catchment and bounding box and how ERA5 data is assumed to overlap the catchment for the Bow at Banff test case.

820 Key assumptions in this part of the workflow are (1) that the user has access to  
 821 the Copernicus Data Store. Instructions on how to obtain access are given in the README  
 822 in folder `./CWARHM/3a_forcing`. (2) We consider that using forcing data that are the  
 823 result of interaction between the atmospheric and land surface model components is un-  
 824 desirable and hence somewhat limit this interaction by downloading certain variables at  
 825 the lowest pressure level instead. (3) ERA5 data points are assumed to be representa-  
 826 tive of grids of size  $0.25^\circ \times 0.25^\circ$ . (4) Gravitational acceleration is assumed to be con-  
 827 stant at  $g = 9.80665 \text{ [m s}^{-2}\text{]}$  (Tiesinga et al., 2019), although in reality this value would  
 828 vary depending on latitude and altitude. (5) ERA5 variable names are changed to more  
 829 descriptive ones that are also the names SUMMA expects these variables to have.

830 *A22.2 Pre-processing of geospatial parameter fields* Pre-processing of geospa-  
 831 tial parameter fields

832 Three different types of geospatial data are required for our example model setup.  
 833 A Digital Elevation Model (DEM) provides the elevation of each HRU and is both a SUMMA  
 834 input and required to apply temperature lapse rates as a preprocessing step. Maps of  
 835 soil classes and vegetation classes are needed to utilize parameter lookup tables. These  
 836 tables specify values for multiple parameters for a variety of soil and land classes. By  
 837 knowing the soil or land class for a given HRU, SUMMA uses the predefined parame-  
 838 ter values for those classes.

839 *Digital Elevation Model* We use the hydrologically adjusted elevations that are  
 840 part of the Merit Hydro dataset (Yamazaki et al., 2019) to determine HRU elevations.  
 841 The Merit Hydro hydrography maps cover the area between  $90^\circ$  North and  $60^\circ$  South  
 842 at a spatial resolution of 3-arc seconds. They are derived from the Merit DEM (Yamazaki  
 843 et al., 2017), which itself is the result of extensive error correction of the SRTM3 (Farr  
 844 et al., 2007) and AW3D-30m (Tadono et al., 2016) DEMs. Scripts can be found in the  
 845 subdirectories of `./CWARHM/3b_parameters/MERIT_Hydro_DEM`.

846 Merit Hydro data are provided as compressed data packages that cover  $30^\circ \times 30^\circ$   
 847 areas. Based on the spatial extent of the domain, as given in the control file, the required  
 848  $30^\circ$  areas are downloaded in compressed format. Data are then uncompressed so that  
 849 the individual GeoTIFF files are accessible. These files are first combined into a Virtual  
 850 Dataset (VRT), from which the exact modeling domain is extracted into a new VRT.  
 851 The VRT with the extracted subdomain is then converted into a single GeoTIFF file that  
 852 contains the DEM for the modeling domain. A key assumption is that the user has ac-  
 853 cess to the MERIT Hydro data. Instructions on how to obtain access are given in the  
 854 README in folder `./CWARHM/3b_parameters/MERIT_Hydro_DEM`.

855 *Vegetation classes* We use MODIS MCD12Q1\_V6 data (Friedl and Sulla-Menashe,  
 856 2019) to determine land cover classes at the HRU level. MODIS MCD12Q1 data are avail-  
 857 able for the years 2001 to 2018 at a 500 m resolution. The data set contains land cover  
 858 classes for multiple different land cover classification schemes. Each data layer is the re-  
 859 sult of supervised classification of MODIS reflectance data (Sulla-Menashe and Friedl,  
 860 2018). Scripts can be found in the subdirectories of `./CWARHM/3b_parameters/MODIS_MCD12Q1_V6`.

861 MODIS MCD12Q1 data is provided as multiple Hierarchical Data Format (HDF)  
 862 files that each cover a part of the planet’s surface at a given time. The source data files  
 863 are in a sinusoidal projection and of irregular shape which makes it difficult to extract  
 864 a specific region. Therefore, the workflow downloads all available individual HDF files  
 865 for each year (i.e., global coverage). The individual files for each data year are combined  
 866 into one Virtual Dataset per year (VRT) for easier processing. Only the data layer of  
 867 interest, the International Geosphere Biosphere Programme (IGBP) land cover classi-  
 868 fication, is included in the VRT. The VRT is reprojected from its original sinusoidal pro-  
 869 jection into a regular latitude/longitude grid (EPSG:4326) from which the modeling do-  
 870 main is extracted. The annual VRTs are then combined into a single multi-band VRT,

871 which is then converted to a multi-band GeoTIFF file. The MODIS documentation ad-  
 872 vises against using the data of an individual year due to data uncertainty (Sulla-Menashe  
 873 and Friedl, 2018). Therefore, the mode land class between 2001 and 2018 is identified  
 874 as the most likely class for each pixel and stored as a new GeoTIFF file.

875 Key assumptions are (1) that the user has access to NASA’s Earth Data website.  
 876 Instructions on how to obtain access are given in the README in folder `./CWARHM/3b_parameters/MODIS_M`  
 877 (2) Our example uses the IGBP land cover classification data, which is one of multiple  
 878 options available.

879 *Soil classes* Our example uses a global map of soil texture classes (Knoben, 2021)  
 880 derived from the SoilGrids 250m dataset (Hengl et al., 2017) to specify representative  
 881 soil classes at the HRU level. The SoilGrids data are provided at a 250 m resolution and  
 882 at seven standard depths (up to 2 m depth). Data are the result of a combination of ap-  
 883 proximately 150,000 observed soil profiles, 158 remote sensing-based soil covariates, and  
 884 multiple machine learning methods. SoilGrids maps of sand, silt, and clay percentages  
 885 were converted to a soil texture map for each depth using the soil texture class bound-  
 886 aries of Benham et al. (2009). For each 250 m map point, the mode soil class of the seven  
 887 soil layers was selected as a representative value for the soil column as a whole, result-  
 888 ing in a single global map of soil texture classes. The pre-processing code needed to cre-  
 889 ate this map (data download, data merge into a coherent map, conversion from percent-  
 890 ages to soil texture, finding the mode of each soil column) is accessible as part of the data  
 891 resource (Knoben, 2021). Scripts can be found in the subdirectories of `./CWARHM/3b_parameters/SOILGRIDS`.

892 The global soil texture class map is provided at the same horizontal resolution as  
 893 the underlying SoilGrids data. The workflow first downloads a map with global cover-  
 894 age. The spatial extent of the modeling domain is extracted based on the bounding box  
 895 specified in the control file and stored as a new GeoTIFF file.

896 Key assumptions are (1) that the user has access to Hydroshare. Instructions on  
 897 how to obtain access are given in the README in folder `./CWARHM/3b_parameters/SOILGRIDS`  
 898 and (2) the global soil map used assumes that mode soil class in each soil column can  
 899 be considered as the representative soil class for the entire soil column and that the soil  
 900 properties (such as saturated conductivity and pore volume) for the mode class are rep-  
 901 resentative of the properties of the column. This approach ignores the existence of lay-  
 902 ered soil profiles and the differences in water movement this can cause (e.g., Vanderborght  
 903 et al., 2005). This also assumes that the most common class contains the layers that are  
 904 most hydrologically active and relevant for modeling purposes.

### 905 ***A23 Mapping of data to model elements***

906 This section provides details about the mapping of preprocessed forcing data onto  
 907 model elements (shown in the intermediate grey shade in Figure 2). This process can-  
 908 not be called truly model-agnostic because whether it is needed depends on the model  
 909 in question: some models are able to ingest the pre-processed data directly.

910 *A23.1 Geospatial parameter fields* In our example, geospatial data in the form  
 911 of GeoTIFF files containing the DEM, land classes, and vegetation classes cannot be in-  
 912 gested by the hydrologic model directly. The data must be mapped onto the model el-  
 913 ements (HRUs) as delineated in the catchment’s shapefile. These procedures use the open-  
 914 source QGIS project (QGIS Development Team, 2021) to provide the necessary Python  
 915 functions (`./CWARHM/4b_remapping/1_topo`). Key assumptions are (1) that MERIT  
 916 Hydrologically Adjusted Elevation data need to be aggregated into mean elevation val-  
 917 ues per model element, whereas (2) soil and vegetation classes need to be aggregated into  
 918 histograms that summarize the distribution of values per model element.

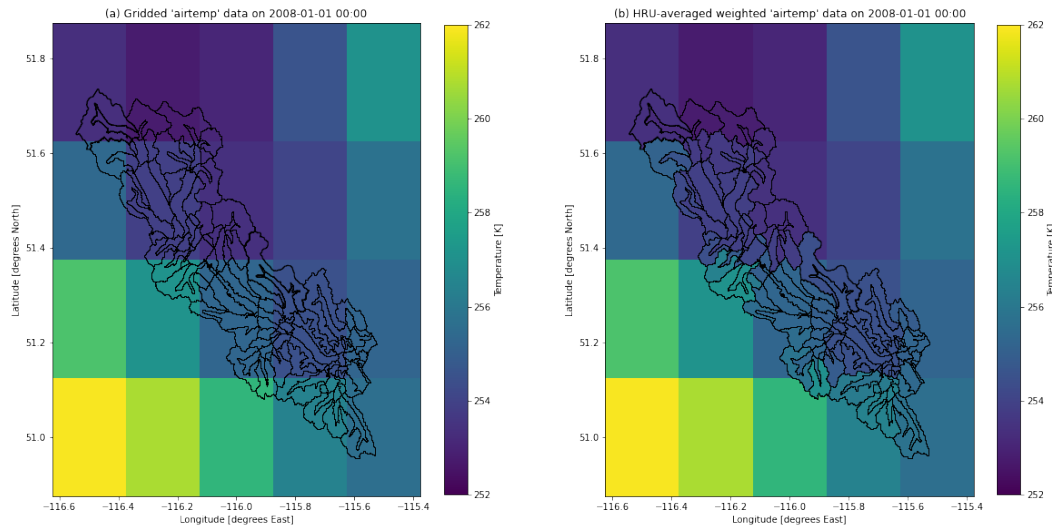


**Figure A3.** (a) Original gridded air temperature data as found in the ERA5 data. (b) HRU-averaged air temperature obtained as a weighted average of the relative contributions of each ERA5 grid cell to each HRU. Temperatures shown outside the catchment boundaries are the original gridded values.

919 *A23.2 Forcing data* Figure 10 shows the original gridded air temperature val-  
 920 ues on an arbitrary day and the HRU-averaged values on that same day that are obtained  
 921 by mapping the gridded forcing data onto the model elements. For each model element,  
 922 the relative overlap with each ERA5 grid cell determines the weight with which that forc-  
 923 ing grid cell contributes to the HRU-averaged value. This procedure is applied to all seven  
 924 forcing variables and all time steps to generate HRU-averaged forcing (*./CWARHM/4b-remapping/2\_forcing*).

925 We then apply a constant environmental lapse rate of  $0.0065 \text{ K m}^{-1}$  (Wallace and  
 926 Hobbs, 2006, p. 421) to the HRU-averaged air temperature data to account for any dif-  
 927 ferences between ERA5 data point elevation and mean HRU elevation (Figure 11). To  
 928 avoid excessive data access, the SUMMA-specific variable *data\_step* (which specifies the  
 929 temporal resolution of the forcing data in [s]) is added to each forcing file at the same  
 930 time as lapse rates are applied.

931 Key assumptions are that (1) a temporally and spatially constant lapse rate can  
 932 be used. This is common in gridded analysis but typically not locally accurate (Minder  
 933 et al., 2010). Local lapse rates may be very different from this assumed value, especially  
 934 in complex terrain and at seasonal or hourly time scales (Cullen and Marshall, 2011; Min-  
 935 der et al., 2010). Regionally and temporally variable lapse rates are a possible way to  
 936 improve this part of the workflow (e.g., Dutra et al., 2020) but doing so is beyond the scope  
 937 of this study. (2) The influence of slope and aspect on radiation fluxes is currently not  
 938 accounted for in forcing data preparation.

### 939 *A24 Model-specific workflow elements*

940 This section provides details model-specific steps of the workflow (shown in dark  
 941 grey in Figure 2). These steps form the interface between preprocessed data and mod-  
 942 els.

943 *A24.1 SUMMA and mizuRoute installation* The source code for both SUMMA  
 944 and mizuRoute can be obtained through GitHub (see Section 8.1.1 and 8.1.2). Scripts

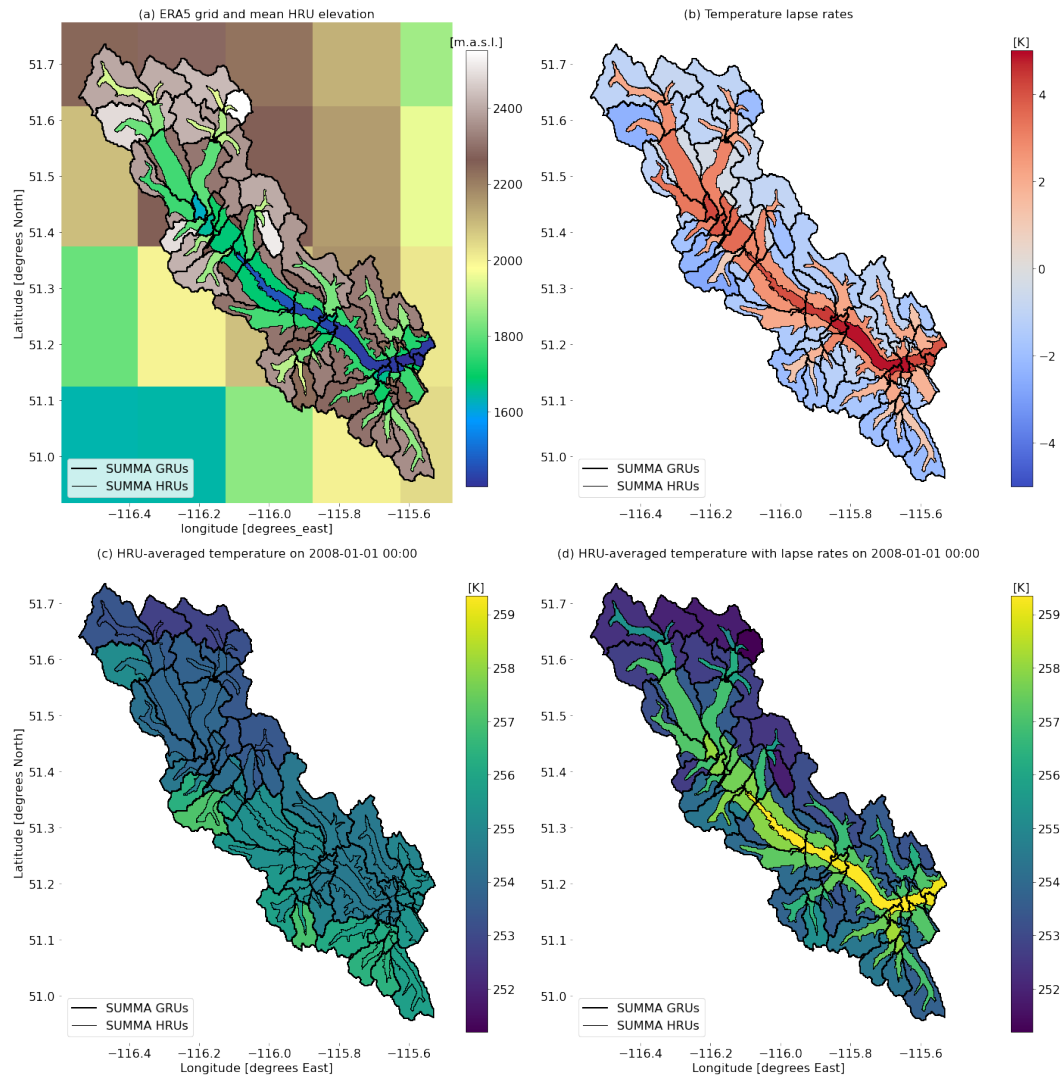


**Figure A4.** (a) HRU-averaged elevation derived from Merit Hydro adjusted elevations data. ERA5 grid point elevation calculated from geopotential data and a spatially constant gravitational acceleration value, visualized as grid cells. (b) Temperature lapse values based on a constant lapse rate and a weighted difference between ERA5 grid point elevation and HRU mean elevation. (c) Air temperature data before lapse rates are applied. (d) Air temperature data after lapse rates are applied.

945 in `./CWARHM/2_install` provide code to download the latest version of both models to  
 946 a local machine. Both models are written in Fortran and need to be compiled to create  
 947 executables. The exact commands and settings needed will vary between different com-  
 948 putational environments. The workflow contains examples of model compile code for a  
 949 specific High Performance Computing environment.

950 Key assumptions are as follows. (1) The user has determined the appropriate set-  
 951 tings to compile both models on their own computational infrastructure and made the  
 952 necessary changes to our provided example code. (2) Both scripts assume that the “de-  
 953 velop” branch of each model is the version of interest. (3) A Linux environment is needed  
 954 for full functionality. A basic alternative that avoids compiling the source code is to in-  
 955 stall pySUMMA and mizuRoute through Conda, but this provides pre-compiled executables  
 956 only. Access to the source code is not possible and updates present on GitHub may  
 957 not immediately appear in the pySUMMA Conda distribution.

958 *A24.2 Shapefile sorting to ensure expected order of model elements* SUMMA makes  
 959 certain assumptions about GRU and HRU order in its input files. These are: (1) GRUs  
 960 and HRUs are in the same order if the forcing files and all SUMMA input files that con-  
 961 tain information at the GRU and HRU level; and (2) HRUs inside a given GRU are found  
 962 at subsequent indices in each NetCDF file. Note that these requirements do not spec-  
 963 ify anything about the values of the GRU and HRU IDs and only focus on the order in  
 964 which the IDs appear in files. The code in `./CWARHM/4a_sort_shape` sorts the shape-  
 965 file that contains the catchment delineation into GRUs and HRUs before this shapefile  
 966 is used by other scripts. This is more efficient than postponing this sorting until the SUMMA  
 967 input files are generated. A key assumption is that computational efficiency is an im-  
 968 portant consideration and therefore this model-specific requirement should be run be-  
 969 fore the (model-agnostic) remapping is performed.

970 *A24.3 SUMMA input files* SUMMA requires several different configuration files:  
 971 1) default parameter values at the GRU and HRU level, 2) *lookup tables* with predefined  
 972 soil and vegetation parameters for different soil and land classes, 3) a *model decisions*  
 973 file that specifies which modeling decisions (e.g., the type of numerical solver) and flux  
 974 parametrizations to use, 4) an *output control* file that specifies which internal model vari-  
 975 ables to write as model output, at which temporal resolution to do so and which, if any,  
 976 summary statistics to provide, 5) a *file manager* that specifies the file paths to all model  
 977 inputs and outputs as well as the time period for the simulation, 6) a *forcing file list* that  
 978 specifies the names of all meteorological forcing files to use, 7) a *trial parameter* file that  
 979 can be used to overrule any parameter value specified in the default parameter files and  
 980 in the lookup tables that can be helpful to quickly test different parameter values dur-  
 981 ing e.g., calibration, 8) an *initial conditions* file that specifies the model states at the be-  
 982 ginning of the first time step, and 9) an *attribute file* that contains topographic infor-  
 983 mation such as elevation, soil type, and land use type at the HRU level.

984 In our example setup, files with default parameter values, lookup tables, model de-  
 985 cisions, and requested outputs are provided as part of the repository. These files do not  
 986 require any information from the preprocessing steps for forcing data and geospatial pa-  
 987 rameter fields and can therefore simply be copied into the new SUMMA settings direc-  
 988 tory. The file manager and forcing file list are populated with information available in  
 989 the workflow control file. The workflow generates a trial parameter file that, for our test  
 990 cases, specifies a required value for only one parameter. This parameter controls the time  
 991 resolution of SUMMA’s simulations and is here specified as 900 seconds (i.e., four times  
 992 smaller than the 1-hourly forcing data resolution) to improve numerical convergence of  
 993 the model equations. The initial conditions file serves a dual purpose: it specifies the model  
 994 states at the start of the simulation and the vertical discretization of the soil domain into  
 995 discrete layers. In this example, SUMMA is initialized with eight soil layers of increas-  
 996 ing thickness (0.025 m for the top layer, 1.50 m for the bottom layer), without any snow

997 or ice present, with some soil and groundwater liquid water storage and at a constant  
 998 temperature of the soil, and canopy domains of 10°C. The attributes file is populated  
 999 with data from the user’s shapefiles (GRU and HRU IDs, HRU-to-GRU mapping, lon-  
 1000 gitude and latitude, HRU area) and from the geospatial preprocessing steps. Figure 12  
 1001 shows the original geospatial parameter fields that are the outcomes of our model-agnostic  
 1002 preprocessing steps and how these are converted into model-specific values for SUMMA’s  
 1003 attributes file. All scripts are available in the subdirectories of *./CWARHM/5\_model\_input/SUMMA*.

1004 Key assumptions are (1) that the HRU and GRU default parameter files, model  
 1005 decisions and lookup table files are assumed to be sensible choices for the domain of in-  
 1006 terest. In particular, the choice of ROSETTA lookup table for soil properties (NCAR  
 1007 Research Applications Laboratory, RAL, 2021; U.S. Department of Agriculture: Agri-  
 1008 cultural Research Service (USDA ARS), 2021) and the modified IGBP table for vege-  
 1009 tation properties (NCAR Research Applications Laboratory, RAL, 2021) inform how the  
 1010 geospatial data is preprocessed (i.e. which geospatial data sets are used and how they  
 1011 are transformed). (2) Vertical discretization of domain is currently set at eight soil lay-  
 1012 ers with increasing thickness with depth. (3) Initial conditions are dry and warm, and  
 1013 there is no snow and ice present in the domain. (3) Model decisions relying on *contourLength*  
 1014 and *tan\_slope* attributes are not supported (currently this is the baseflow model decision  
 1015 *qbaseTopmodel*, as well as certain radiation calculations that account for slope inclina-  
 1016 tion). Attribute variable *downHRUindex* is only used if decision *qbaseTopmodel* is ac-  
 1017 tive and is therefore set to zero.

1018 *A24.4 mizuRoute input files* mizuRoute requires several configuration files: 1)  
 1019 a *default parameter* file that has values for its different routing schemes, 2) a *network*  
 1020 *topology* file that contains a description of the river network and its properties, 3) op-  
 1021 tionally, a *remapping* file that shows how output from a hydrologic model should be mapped  
 1022 onto mizuRoute’s routing network, and 4) a *mizuRoute.control* file that specifies the nec-  
 1023 essary file paths and routing settings. In our example setup, a default routing param-  
 1024 eter file is provided as part of the repository. This file does not require any information  
 1025 from the preprocessing steps for forcing data and geospatial parameter fields and can there-  
 1026 fore simply be copied into the new mizuRoute settings directory. The network topology  
 1027 file contains a description of the routing basins and their associated stream segments.  
 1028 It specifies which basins and segments exist, which segment each basin drains into and  
 1029 physical properties of the domain such as drainage area, segment length and segment  
 1030 slope. The optional remapping file only needs to be used in cases where the hydrologic  
 1031 model operates on model elements that do not map directly onto mizuRoute’s routing  
 1032 basins. In such a case the remapping file specifies the weight with which each hydrologic  
 1033 catchment contributes flow to each routing basin. The *mizuRoute.control* file is popu-  
 1034 lated with information available in the workflow control file. All scripts are available in  
 1035 the subdirectories of *./CWARHM/5\_model\_input/mizuRoute*.

1036 Key assumptions are (1) that the provided routing parameter values are appropri-  
 1037 ate for the domain and (2) Hillslope routing (i.e. routing between different SUMMA HRUs  
 1038 inside a given SUMMA GRU) is performed by SUMMA. mizuRoute is configured to do  
 1039 the river network routing between different SUMMA GRUs.

1040 *A24.5 Model runs* Model runs use the compiled SUMMA and mizuRoute ex-  
 1041 ecutables to perform simulations using the inputs and settings defined in their respec-  
 1042 tive configuration files (*./CWARHM/6\_model\_runs*). As part of the model run scripts,  
 1043 model configuration files are copied into the simulations output directories. This ensures  
 1044 traceability of the simulations by keeping a record of the settings used to generate the  
 1045 simulations.

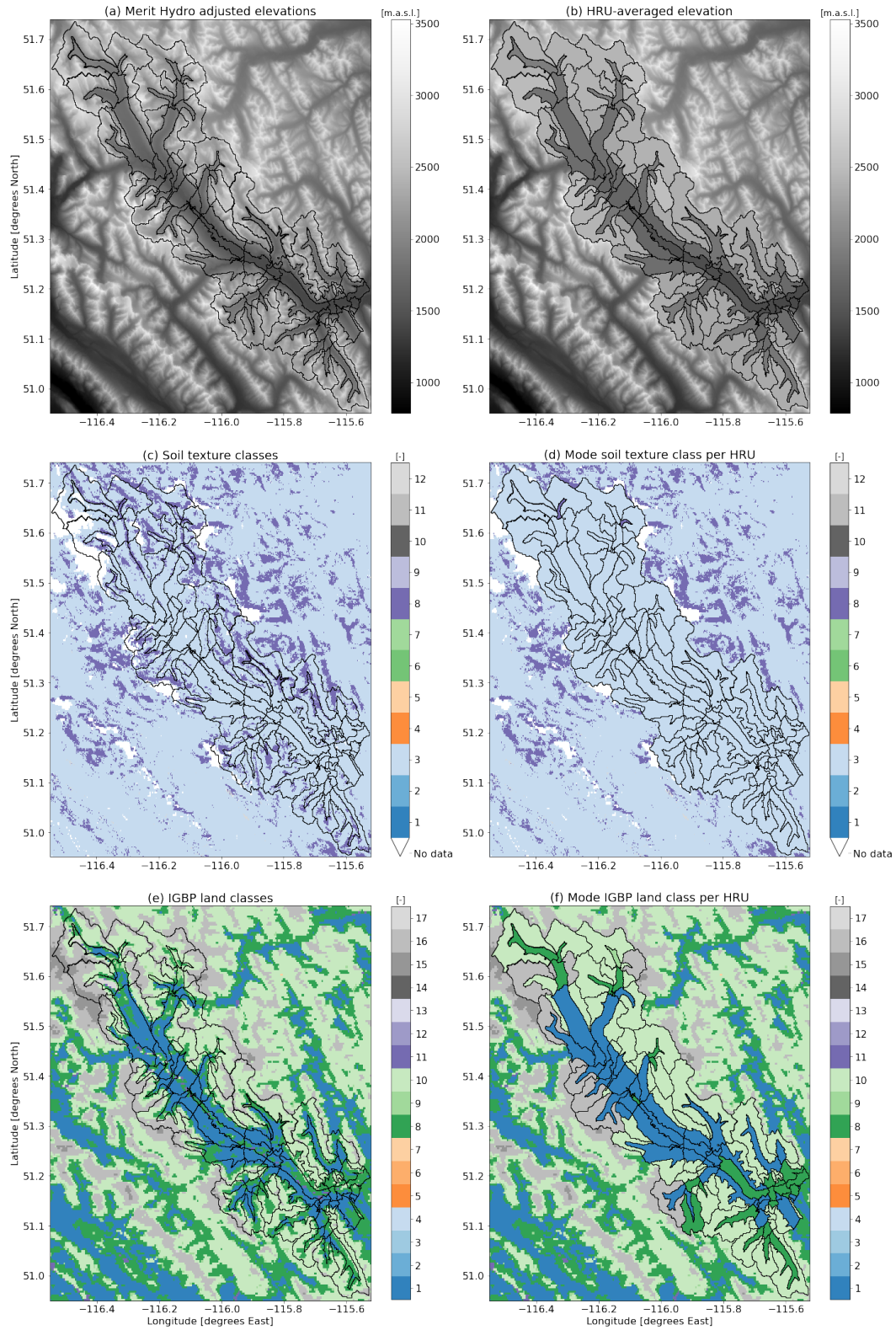


**Figure A5.** Mapping of geospatial parameter fields onto model elements. (a, b) MERIT Hydro adjusted elevations DEM source data and the mean elevation per HRU. (c, d) Soil texture classes derived from SOILGRIDS sand, silt and clay percentages and the most common class per HRU. (e, f) IGBP land classes from MODIS data and the most common class per HRU.

1046 **A25 Post-processing**

1047 Post-processing of model results in this example is limited to the code needed to  
1048 generate the modeling domain figure in this manuscript (`./CWARHM/7_visualization`).  
1049 Further visualization code may be added over time, as such code is created for specific  
1050 experiments.

1051 **Appendix B Note on data accuracy**

1052 Our example workflow uses ERA5 forcing data, Merit Hydro DEM, SOILGRIDS-  
1053 derived soil texture classes, and MODIS IGBP land classes for their global coverage. This  
1054 enables global applications of the workflow. Such global datasets are based on a com-  
1055 bination of observations and geospatial data processing methods to estimate data val-  
1056 ues for locations where no observations are available. These approaches may need to sac-  
1057 rifice local information content for global coverage and are not always able to utilize the  
1058 most accurate local data available.

1059 ERA5 is a reanalysis product from a data assimilating numerical weather predic-  
1060 tion model. ERA5 precipitation estimates compare favorably to other global products  
1061 at a daily resolution (Beck et al., 2019) but are typically not as accurate as local gauge  
1062 or radar-based observations, especially in regions with complex topography (e.g., Am-  
1063 jad et al., 2020; Jiang et al., 2021; Tang et al., 2020; Xu et al., 2019). Jiang et al. (2020)  
1064 show a similar reduced accuracy of ERA5 compared to station observations for direct  
1065 and diffuse solar radiation estimates. Less is known about the accuracy of the remain-  
1066 ing ERA5 forcing variables used in our workflow, and it is possible that the relatively  
1067 coarse resolution of ERA5 data means that these variables may not be as accurate as  
1068 local products.

1069 The MERIT Hydro hydrologically adjusted elevation dataset (Yamazaki et al., 2019)  
1070 is based on the MERIT DEM (Yamazaki et al., 2017), which itself is the result of ap-  
1071 plying an error-removal algorithm to existing space-borne DEMs. It is available glob-  
1072 ally at approximately 90 m spatial resolution. The MERIT Hydro data represent an ad-  
1073 vance over earlier products such as HydroSheds (Lehner et al., 2008), especially at higher  
1074 latitudes, but some uncertainty in the produced hydrography data remains in regions  
1075 with low topographic variation, with endorheic basins, with seasonally varying connec-  
1076 tivity, and with channel bifurcations. The MERIT Hydro hydrologically adjusted ele-  
1077 vations are a modification of the MERIT DEM that satisfies the condition “downstream  
1078 pixels are not higher than upstream pixels”. This procedure relies on a combination of  
1079 correctly identifying endorheic basins, connections between sub-basins, and adjusting pixel  
1080 elevations to create continuous flow paths. It is unknown to what extent this procedure  
1081 affects the mean catchment elevation we derive from the hydrologically adjusted eleva-  
1082 tion. It is plausible that mean catchment elevations derived from this data will be less  
1083 accurate in regions with rapidly varying topography, where catchment slopes are steep  
1084 compared to the MERIT Hydro resolution.

1085 The SoilGrids database uses observations of approximately 150,000 soil profiles, pseudo-  
1086 observations that encode expert knowledge in a similar way to actual observed soil pro-  
1087 files, and machine learning to provide global estimates of various soil properties at a 250  
1088 m resolution. Ten-fold cross-validation of the resulting sand, silt, and clay percentage  
1089 data used in our workflow shows that this approach explains approximately 75% of the  
1090 variation in these soil properties. There is no systematic over or under prediction of these  
1091 properties, but large differences between estimates and observations exist nonetheless  
1092 in certain cases (Hengl et al., 2017).

1093 MODIS MCD12Q1\_v6 data uses a combination of random forests, bias and error  
1094 correction based on ancillary data, and a hidden Markov Model approach to convert pre-  
1095 processed satellite reflectance imagery into land cover classification categories. Ten-fold

1096 cross-validation of the resulting classification indicates that the IGBP classes used in our  
 1097 workflow are accurate in approximately two-thirds of cases. Misclassifications tend to  
 1098 occur in regions that contain substantial land cover variability at scales smaller than the  
 1099 500 m MODIS resolution is provided at and along climatic gradients where the cover type  
 1100 changes gradually (Sulla-Menashe et al., 2019).

1101 We therefore recommend that users replace our chosen global data products with  
 1102 more appropriate local data if such data are available and the project scope lies within  
 1103 the data domain. Due to the modular nature of the workflow, this replacement requires  
 1104 only minimal changes to the model configuration code. In terms of Figure 9, incorpo-  
 1105 rating a different data set would require a new data-specific pre-processing module for  
 1106 which our existing workflow can serve as a guide. We emphasize that this workflow is  
 1107 intended to provide a baseline configuration upon which a user can improve. Our work-  
 1108 flow does not contain any elements that compare the resulting simulations to observa-  
 1109 tions to ascertain the quality of these simulations. A model setup generated through this  
 1110 workflow should thus not be assumed to be fit for a given purpose, unless shown to be  
 1111 so by the user’s own model evaluation procedures.

## 1112 Open Research

1113 The latest version of the workflow code presented in this study is available on [https://](https://github.com/CH-Earth/CWARHM)  
 1114 [github.com/CH-Earth/CWARHM](https://github.com/CH-Earth/CWARHM) with the specific version used to generate Figures 7, 8,  
 1115 10-14 via DOI, accessible under GNU GPL v3.0. **Note to reviewers: we intend to**  
 1116 **mint a DOI once the peer review process is complete**

1117 The SUMMA (Clark et al., 2015a, 2015b, 2021c) version used for simulations in  
 1118 this paper can be identified by Git commit ID 3d17543 (North America domain and Bow  
 1119 at Banff domain). Source code accessible on: <https://github.com/CH-Earth/summa>

1120 The mizuRoute (Mizukami et al., 2021, 2016) version used for simulations in this  
 1121 paper can be identified by Git commit ID c2de53d (North America domain) and Git com-  
 1122 mit ID d43066b (Bow at Banff domain). Source code accessible on: [https://github.com/](https://github.com/ESCOMP/mizuRoute)  
 1123 [ESCOMP/mizuRoute](https://github.com/ESCOMP/mizuRoute)

1124 The single level ERA5 data (Hersbach et al., 2018) used as meteorological model  
 1125 input data are available at the Copernicus Climate Change Service (C3S) Climate Data  
 1126 Store (CDS) via <https://dx.doi.org/10.24381/cds.adbb2d47> under the *Licence to*  
 1127 *use Copernicus Products* ([https://cds.climate.copernicus.eu/api/v2/terms/static/](https://cds.climate.copernicus.eu/api/v2/terms/static/licence-to-use-copernicus-products.pdf)  
 1128 [licence-to-use-copernicus-products.pdf](https://cds.climate.copernicus.eu/api/v2/terms/static/licence-to-use-copernicus-products.pdf); last access 2021-11-04).

1129 The pressure level ERA5 data (Hersbach et al., 2017) used as meteorological model  
 1130 input data are available at the Copernicus Climate Change Service (C3S) Climate Data  
 1131 Store (CDS) via MARS request (no DOI) under *Licence to use Copernicus Products* ([https://](https://cds.climate.copernicus.eu/api/v2/terms/static/licence-to-use-copernicus-products.pdf)  
 1132 [cds.climate.copernicus.eu/api/v2/terms/static/licence-to-use-copernicus-](https://cds.climate.copernicus.eu/api/v2/terms/static/licence-to-use-copernicus-products.pdf)  
 1133 [products](https://cds.climate.copernicus.eu/api/v2/terms/static/licence-to-use-copernicus-products.pdf)  
 1134 [.pdf](https://cds.climate.copernicus.eu/api/v2/terms/static/licence-to-use-copernicus-products.pdf); last access 2021-11-04). Data downloaded on 2021-04-17 for Bow at Banff test case;  
 between 2020-11-14 and 2020-12-23 for North America test case.

1135 The MERIT Hydro Hydrologically Adjusted Elevations (Yamazaki et al., 2019) used  
 1136 as Digital Elevation Model to determine mean catchment elevations is available at [http://](http://hydro.iis.u-tokyo.ac.jp/~yamadai/MERIT_Hydro/)  
 1137 [hydro.iis.u-tokyo.ac.jp/~yamadai/MERIT\\_Hydro/](http://hydro.iis.u-tokyo.ac.jp/~yamadai/MERIT_Hydro/) (last webpage access on 2021-11-  
 1138 04) as version v1.0.1 (no DOI available; data downloaded on 2021-04-17 for Bow at Banff  
 1139 test case, 2021-05-15 for North America test case), accessible under CC-BY-NC 4.0 or  
 1140 ODbL 1.0.

1141 The MODIS MCD12Q1 V6 data (Friedl and Sulla-Menashe, 2019; Sulla-Menashe  
 1142 and Friedl, 2018) used to find a representative IGBP land cover class for each model el-

1143 element is available at the NASA EOSDIS Land Processes DAAC via [https://dx.doi](https://dx.doi.org/10.5067/MODIS/MCD12Q1.006)  
 1144 [.org/10.5067/MODIS/MCD12Q1.006](https://dx.doi.org/10.5067/MODIS/MCD12Q1.006), with no restrictions on reuse, sale or redistribution.

1145 The Global USDA-NRCS soil texture class map (Knoben, 2021) derived from the  
 1146 Soilgrids250m data set (Hengl et al., 2017) and used to find a representative USGS soil  
 1147 type class for each model element is available as a Hydroshare resource via [https://dx](https://dx.doi.org/10.4211/hs.1361509511e44adfba814f6950c6e742)  
 1148 [.doi.org/10.4211/hs.1361509511e44adfba814f6950c6e742](https://dx.doi.org/10.4211/hs.1361509511e44adfba814f6950c6e742), under ODbL v1.0.

1149 The shapefile that contains the catchment delineation for the Bow At Banff test  
 1150 case is derived from the MERIT Hydro basins data set (Lin et al., 2019) and available  
 1151 as part of the workflow repository. The shapefile that contains the catchment delineation  
 1152 for the North America test case is derived from the MERIT Hydro basins data set, and  
 1153 ... **Note to reviewers: we are in the processing of ensuring that this shape-**  
 1154 **file will be publicly available.**

## 1155 Acknowledgements

1156 We are thankful for the contributions of Guoqiang Tang, who confirmed that our  
 1157 code is functional on macOS and the general comments for workflow improvement given  
 1158 by Guoqiang Tang, Dave Casson, Hongli Liu, Jim Freer and Hannah Burdett. We are  
 1159 also thankful for the efforts of Reza Zolfaghari and Kyle Klenk who assisted in under-  
 1160 standing and solving specific numerical issues, and to Louise Arnal for feedback on the  
 1161 workflow schematics. Wouter Knoben, Martyn Clark, Shervan Gharari, Chris Marsh and  
 1162 Ray Spiteri were supported by the Global Water Futures program, University of Saskatchewan.  
 1163 The work of David Tarboton was supported by the US National Science Foundation un-  
 1164 der collaborative grants ICER 1928369 and OAC 1835569. The work of Jerad Bales was  
 1165 supported by NSF grant EAR 1849458. NCAR co-author contributions were supported  
 1166 by the US Army Corps of Engineers Responses to Climate Change program and the US  
 1167 Bureau of Reclamation under Cooperative Agreement R16AC00039.

## 1168 References

- 1169 Amjad, M., Yilmaz, M.T., Yucel, I., Yilmaz, K.K., 2020. Performance evaluation of satellite-  
 1170 and model-based precipitation products over varying climate and complex topography.  
 1171 *J. Hydrol.* 584, 124707. <https://doi.org/10.1016/j.jhydrol.2020.124707>
- 1172 Añel, J.A., 2017. Comment on “Most computational hydrology is not reproducible, so  
 1173 is it really science?” by Christopher Hutton et al.: NECESSARY CONDITIONS FOR  
 1174 REPRODUCIBILITY. *Water Resour. Res.* 53, 2572–2574. <https://doi.org/10.1002/2016WR020190>
- 1175 Archfield, S.A., Clark, M., Arheimer, B., Hay, L.E., McMillan, H., Kiang, J.E., Seibert,  
 1176 J., Hakala, K., Bock, A., Wagener, T., Farmer, W.H., Andréassian, V., Attinger, S., Viglione,  
 1177 A., Knight, R., Markstrom, S., Over, T., 2015. Accelerating advances in continental do-  
 1178 main hydrologic modeling. *Water Resour. Res.* 51, 10078–10091. <https://doi.org/10.1002/2015WR017498>
- 1179 Arsenault, R., Poulin, A., Côté, P., Brissette, F., 2014. Comparison of Stochastic Op-  
 1180 timization Algorithms in Hydrological Model Calibration. *J. Hydrol. Eng.* 19, 1374–1384.  
 1181 [https://doi.org/10.1061/\(ASCE\)HE.1943-5584.0000938](https://doi.org/10.1061/(ASCE)HE.1943-5584.0000938)
- 1182 Bandaragoda, C., Castronova, A., Istanbuluoglu, E., Strauch, R., Nudurupati, S.S., Phuong,  
 1183 J., Adams, J.M., Gasparini, N.M., Barnhart, K., Hutton, E.W.H., Hobley, D.E.J., Lyons,  
 1184 N.J., Tucker, G.E., Tarboton, D.G., Idaszak, R., Wang, S., 2019. Enabling Collabora-  
 1185 tive Numerical Modeling in Earth Sciences using Knowledge Infrastructure. *Environ. Model.*  
 1186 *Softw.* 120, 104424. <https://doi.org/10.1016/j.envsoft.2019.03.020>
- 1187 Bast, R., 2019. A FAIRer future. *Nat. Phys.* 15, 728–730. [https://doi.org/10.1038/s41567-](https://doi.org/10.1038/s41567-019-0624-3)  
 1188 [019-0624-3](https://doi.org/10.1038/s41567-019-0624-3)

- 1189 Bavay, M., Reisecker, M., Egger, T., Korhammer, D., 2020. Inishell 2.0: Semantically  
1190 driven automatic GUI generation for scientific models (preprint). *Hydrology*. [https://doi.org/10.5194/gmd-](https://doi.org/10.5194/gmd-2020-339)  
1191 [2020-339](https://doi.org/10.5194/gmd-2020-339)
- 1192 Beck, H.E., Pan, M., Roy, T., Weedon, G.P., Pappenberger, F., van Dijk, A.I.J.M., Huff-  
1193 man, G.J., Adler, R.F., Wood, E.F., 2019. Daily evaluation of 26 precipitation datasets  
1194 using Stage-IV gauge-radar data for the CONUS. *Hydrol. Earth Syst. Sci.* 23, 207–224.  
1195 <https://doi.org/10.5194/hess-23-207-2019>
- 1196 Benham, E., Ahrens, R.J., Nettleton, W.D., 2009. Clarification of Soil Texture Class Bound-  
1197 aries.
- 1198 Bennett, A., Hamman, J., Nijssen, B., 2020. MetSim: A Python package for estimation  
1199 and disaggregation of meteorological data. *J. Open Source Softw.* 5, 2042. <https://doi.org/10.21105/joss.02042>
- 1200 Blair, G.S., Beven, K., Lamb, R., Bassett, R., Cauwenberghs, K., Hankin, B., Dean, G.,  
1201 Hunter, N., Edwards, L., Nundloll, V., Samreen, F., Simm, W., Towe, R., 2019. Mod-  
1202 els of everywhere revisited: A technological perspective. *Environ. Model. Softw.* 122,  
1203 104521. <https://doi.org/10.1016/j.envsoft.2019.104521>
- 1204 Blodgett, D., Dornblut, I., 2018. OGC® WaterML 2: Part 3 - Surface Hydrology Fea-  
1205 tures (HY\_Features) - Conceptual Model [WWW Document]. URL [http://docs.openeospatial.org/is/14-](http://docs.openeospatial.org/is/14-111r6/14-111r6.html#_catchment_area)  
1206 [111r6/14-111r6.html#\\_catchment\\_area](http://docs.openeospatial.org/is/14-111r6/14-111r6.html#_catchment_area) (accessed 12.2.21).
- 1207 Blöschl, G., Bárdossy, A., Koutsoyiannis, D., Kundzewicz, Z.W., Littlewood, I., Mon-  
1208 tanari, A., Savenije, H., 2014. On the future of journal publications in hydrology. *Wa-*  
1209 *ter Resour. Res.* 50, 2795–2797. <https://doi.org/10.1002/2014WR015613>
- 1210 Bock, a. R., Hay, L.E., McCabe, G.J., Markstrom, S.L., Atkinson, R.D., 2015. Param-  
1211 eter regionalization of a monthly water balance model for the conterminous United States.  
1212 *Hydrol. Earth Syst. Sci. Discuss.* 12, 10023–10066. [https://doi.org/10.5194/hessd-12-](https://doi.org/10.5194/hessd-12-10023-2015)  
1213 [10023-2015](https://doi.org/10.5194/hessd-12-10023-2015)
- 1214 Chaney, N., Fisher, C., 2021. chaneyn/geospatialtools: geospatialtools\_nov2021. Zen-  
1215 odo. <https://doi.org/10.5281/ZENODO.5676031>
- 1216 Choi, Y.-D., Goodall, J.L., Sadler, J.M., Castronova, A.M., Bennett, A., Li, Z., Nijssen,  
1217 B., Wang, S., Clark, M.P., Ames, D.P., Horsburgh, J.S., Yi, H., Bandaragoda, C., Seul,  
1218 M., Hooper, R., Tarboton, D.G., 2021. Toward open and reproducible environmental mod-  
1219 eling by integrating online data repositories, computational environments, and model Ap-  
1220 plication Programming Interfaces. *Environ. Model. Softw.* 135, 104888. <https://doi.org/10.1016/j.envsoft.2020.10>
- 1221 Chuah, J., Deeds, M., Malik, T., Choi, Y., Goodall, J.L., 2020. Documenting Comput-  
1222 ing Environments for Reproducible Experiments, in: *Parallel Computing: Technology*  
1223 *Trends, Advances in Parallel Computing*. IOS Press, Amsterdam, Netherlands, pp. 756–  
1224 765.
- 1225 Clark, M.P., Luce, C.H., AghaKouchak, A., Berghuijs, W., David, C.H., Duan, Q., Ge,  
1226 S., van Meerveld, I., Zheng, C., Parlange, M.B., Tyler, S.W., 2021a. Open Science: Open  
1227 Data, Open Models, ... and Open Publications? *Water Resour. Res.* 57. <https://doi.org/10.1029/2020WR029480>
- 1228 Clark, M.P., Nijssen, B., Lundquist, J.D., Kavetski, D., Rupp, D.E., Woods, R.A., Freer,  
1229 J.E., Gutmann, E.D., Wood, A.W., Brekke, L.D., Arnold, J.R., Gochis, D.J., Rasmussen,  
1230 R.M., 2015a. A unified approach for process-based hydrologic modeling: 1. Modeling con-  
1231 cept. *Water Resour. Res.* 51, 2498–2514. <https://doi.org/10.1002/2015WR017198>
- 1232 Clark, M.P., Nijssen, B., Lundquist, J.D., Kavetski, D., Rupp, D.E., Woods, R.A., Freer,  
1233 J.E., Gutmann, E.D., Wood, A.W., Gochis, D.J., Rasmussen, R.M., Tarboton, D.G., Ma-  
1234 hat, V., Flerchinger, G.N., Marks, D.G., 2015b. A unified approach for process-based

- 1235 hydrologic modeling: 2. Model implementation and case studies. *Water Resour. Res.* 51,  
1236 2515–2542. <https://doi.org/10.1002/2015WR017200>
- 1237 Clark, M.P., Vogel, R.M., Lamontagne, J.R., Mizukami, N., Knoben, W.J.M., Tang, G.,  
1238 Gharari, S., Freer, J.E., Whitfield, P.H., Shook, K.R., Papalexiou, S.M., 2021b. The Abuse  
1239 of Popular Performance Metrics in Hydrologic Modeling. *Water Resour. Res.* 57. <https://doi.org/10.1029/2020WJ>
- 1240 Clark, M.P., Zolfaghari, R., Green, K.R., Trim, S., Knoben, W.J.M., Bennett, A., Ni-  
1241 jssen, B., Ireson, A., Spiteri, R.J., 2021c. The numerical implementation of land mod-  
1242 els: Problem formulation and laugh tests. *J. Hydrometeorol.* [https://doi.org/10.1175/JHM-](https://doi.org/10.1175/JHM-D-20-0175.1)  
1243 [D-20-0175.1](https://doi.org/10.1175/JHM-D-20-0175.1)
- 1244 Copernicus Climate Change Service (C3S), 2017. ERA5: Fifth generation of ECMWF  
1245 atmospheric reanalyses of the global climate.
- 1246 Cullen, R.M., Marshall, S.J., 2011. Mesoscale Temperature Patterns in the Rocky Moun-  
1247 tains and Foothills Region of Southern Alberta. *Atmosphere-Ocean* 49, 189–205. <https://doi.org/10.1080/0705590>
- 1248 Dutra, E., Muñoz-Sabater, J., Bousssetta, S., Komori, T., Hirahara, S., Balsamo, G., 2020.  
1249 Environmental Lapse Rate for High-Resolution Land Surface Downscaling: An Appli-  
1250 cation to ERA5. *Earth Space Sci.* 7. <https://doi.org/10.1029/2019EA000984>
- 1251 Essawy, B.T., Goodall, J.L., Voce, D., Morsy, M.M., Sadler, J.M., Choi, Y.D., Tarboton,  
1252 D.G., Malik, T., 2020. A taxonomy for reproducible and replicable research in environ-  
1253 mental modelling. *Environ. Model. Softw.* 134, 104753. <https://doi.org/10.1016/j.envsoft.2020.104753>
- 1254 Essawy, B.T., Goodall, J.L., Xu, H., Rajasekar, A., Myers, J.D., Kugler, T.A., Billah,  
1255 M.M., Whitton, M.C., Moore, R.W., 2016. Server-side workflow execution using data  
1256 grid technology for reproducible analyses of data-intensive hydrologic systems. *Earth Space*  
1257 *Sci.* 3, 163–175. <https://doi.org/10.1002/2015EA000139>
- 1258 Famiglietti, J.S., Murdoch, L., Lakshmi, V., Arrigo, J., Hooper, R., 2011. Establishing  
1259 a Framework for Community Modeling in Hydrologic Science, Report from the 3rd Work-  
1260 shop on a Community Hydrologic Modeling Platform (CHyMP): A Strategic and Im-  
1261 plementation Plan. Beckman Center of the National Academies, University of Califor-  
1262 nia at Irvine.
- 1263 Farr, T.G., Rosen, P.A., Caro, E., Crippen, R., Duren, R., Hensley, S., Kobrick, M., Paller,  
1264 M., Rodriguez, E., Roth, L., Seal, D., Shaffer, S., Shimada, J., Umland, J., Werner, M.,  
1265 Oskin, M., Burbank, D., Alsdorf, D., 2007. The Shuttle Radar Topography Mission. *Rev.*  
1266 *Geophys.* 45, RG2004. <https://doi.org/10.1029/2005RG000183>
- 1267 Friedl, M., Sulla-Menashe, D., 2019. MCD12Q1 MODIS/Terra+Aqua Land Cover Type  
1268 Yearly L3 Global 500m SIN Grid V006. <https://doi.org/10.5067/MODIS/MCD12Q1.006>
- 1269 Gan, T., Tarboton, D.G., Dash, P., Gichamo, T.Z., Horsburgh, J.S., 2020. Integrating  
1270 hydrologic modeling web services with online data sharing to prepare, store, and exe-  
1271 cute hydrologic models. *Environ. Model. Softw.* 130, 104731. <https://doi.org/10.1016/j.envsoft.2020.104731>
- 1272 Gharari, S., Clark, M.P., Mizukami, N., Knoben, W.J.M., Wong, J.S., Pietroniro, A., 2020.  
1273 Flexible vector-based spatial configurations in land models. *Hydrol. Earth Syst. Sci.* 24,  
1274 5953–5971. <https://doi.org/10.5194/hess-24-5953-2020>
- 1275 Gichamo, T.Z., Sazib, N.S., Tarboton, D.G., Dash, P., 2020. HydroDS: Data services in  
1276 support of physically based, distributed hydrological models. *Environ. Model. Softw.*  
1277 125, 104623. <https://doi.org/10.1016/j.envsoft.2020.104623>
- 1278 Gil, Y., David, C.H., Demir, I., Essawy, B.T., Fulweiler, R.W., Goodall, J.L., Karlstrom,  
1279 L., Lee, H., Mills, H.J., Oh, J., Pierce, S.A., Pope, A., Tzeng, M.W., Villamizar, S.R.,  
1280 Yu, X., 2016. Toward the Geoscience Paper of the Future: Best practices for document-

- 1281 ing and sharing research from data to software to provenance. *Earth Space Sci.* 3, 388–  
1282 415. <https://doi.org/10.1002/2015EA000136>
- 1283 Gupta, H.V., Wagener, T., Liu, Y., 2008. Reconciling theory with observations: elements  
1284 of a diagnostic approach to model evaluation. *Hydrol. Process.* 3813, 3802–3813. <https://doi.org/10.1002/hyp.698>
- 1285 Hamman, J.J., Nijssen, B., Bohn, T.J., Gergel, D.R., Mao, Y., 2018. The Variable In-  
1286 filtration Capacity model version 5 (VIC-5): infrastructure improvements for new ap-  
1287 plications and reproducibility. *Geosci. Model Dev.* 11, 3481–3496. <https://doi.org/10.5194/gmd-11-3481-2018>
- 1289 Havens, S., Marks, D., Sandusky, M., Hedrick, A., Johnson, M., Robertson, M., Trujillo,  
1290 E., 2020. Automated Water Supply Model (AWSM): Streamlining and standardizing ap-  
1291 plication of a physically based snow model for water resources and reproducible science.  
1292 *Comput. Geosci.* 144, 104571. <https://doi.org/10.1016/j.cageo.2020.104571>
- 1293 Hengl, T., Mendes de Jesus, J., Heuvelink, G.B.M., Ruiperez Gonzalez, M., Kilibarda,  
1294 M., Blagotić, A., Shangguan, W., Wright, M.N., Geng, X., Bauer-Marschallinger, B., Gue-  
1295 varra, M.A., Vargas, R., MacMillan, R.A., Batjes, N.H., Leenaars, J.G.B., Ribeiro, E.,  
1296 Wheeler, I., Mantel, S., Kempen, B., 2017. SoilGrids250m: Global gridded soil informa-  
1297 tion based on machine learning. *PLOS ONE* 12, e0169748. <https://doi.org/10.1371/journal.pone.0169748>
- 1298 Hersbach, H., Bell, B., Berrisford, P., Biavati, G., Horányi, A., Muñoz Sabater, J., Nico-  
1299 las, J., Peubey, C., Radu, R., Rozum, I., Schepers, D., Simmons, A., Soci, C., Dee, D.,  
1300 Thépaut, J.-N., 2018. ERA5 hourly data on single levels from 1979 to present. <https://doi.org/10.24381/cds.adbb>
- 1301 Hersbach, H., Bell, B., Berrisford, P., Hirahara, S., Horányi, A., Muñoz-Sabater, J., Nico-  
1302 las, J., Peubey, C., Radu, R., Schepers, D., Simmons, A., Soci, C., Abdalla, S., Abellan,  
1303 X., Balsamo, G., Bechtold, P., Biavati, G., Bidlot, J., Bonavita, M., Chiara, G., Dahlgren,  
1304 P., Dee, D., Diamantakis, M., Dragani, R., Flemming, J., Forbes, R., Fuentes, M., Geer,  
1305 A., Haimberger, L., Healy, S., Hogan, R.J., Hólm, E., Janisková, M., Keeley, S., Laloy-  
1306 aux, P., Lopez, P., Lupu, C., Radnoti, G., Rosnay, P., Rozum, I., Vamborg, F., Villaume,  
1307 S., Thépaut, J., 2020. The ERA5 global reanalysis. *Q. J. R. Meteorol. Soc.* 146, 1999–  
1308 2049. <https://doi.org/10.1002/qj.3803>
- 1309 Hersbach, H., Bell, B., Berrisford, P., Hirahara, S., Horányi, A., Muñoz-Sabater, J., Nico-  
1310 las, J., Peubey, C., Radu, R., Schepers, D., Simmons, A., Soci, C., Abdalla, S., Abellan,  
1311 X., Balsamo, G., Bechtold, P., Biavati, G., Bidlot, J., Bonavita, M., De Chiara, G., Dahlgren,  
1312 P., Dee, P., Diamantakis, M., Dragani, R., Flemming, J., Forbes, R., Fuentes, M., Geer,  
1313 A., Haimberger, L., Healy, S., Hogan, R.J., Hólm, E., Janisková, M., Keeley, S., Laloy-  
1314 aux, P., Lopez, P., Lupu, C., Radnoti, G., de Rosnay, P., Rozum, I., Vamborg, F., Vil-  
1315 laume, S., Thépaut, J.-N., 2017. Complete ERA5: Fifth generation of ECMWF atmo-  
1316 spheric reanalyses of the global climate.
- 1317 Husain, S.Z., Alavi, N., Bélair, S., Carrera, M., Zhang, S., Fortin, V., Abrahamowicz,  
1318 M., Gauthier, N., 2016. The Multibudget Soil, Vegetation, and Snow (SVS) Scheme for  
1319 Land Surface Parameterization: Offline Warm Season Evaluation. *J. Hydrometeorol.* 17,  
1320 2293–2313. <https://doi.org/10.1175/JHM-D-15-0228.1>
- 1321 Hut, R.W., van de Giesen, N.C., Drost, N., 2017. Comment on “Most computational hy-  
1322 drology is not reproducible, so is it really science?” by Christopher Hutton et al.: Let  
1323 hydrologists learn the latest computer science by working with Research Software En-  
1324 gineers (RSEs) and not reinvent the waterwheel ourselves. *Water Resour. Res.* 53, 4524–  
1325 4526. <https://doi.org/10.1002/2017WR020665>
- 1326 Hutton, C., Wagener, T., Freer, J., Han, D., Duffy, C., Arheimer, B., 2016. Most com-  
1327 putational hydrology is not reproducible, so is it really science? *Water Resour. Res.* 52,  
1328 7548–7555. <https://doi.org/10.1002/2016WR019285>

- 1329 Jiang, H., Yang, Y., Bai, Y., Wang, H., 2020. Evaluation of the Total, Direct, and Dif-  
 1330 fuse Solar Radiations From the ERA5 Reanalysis Data in China. *IEEE Geosci. Remote*  
 1331 *Sens. Lett.* 17, 47–51. <https://doi.org/10.1109/LGRS.2019.2916410>
- 1332 Jiang, Q., Li, W., Fan, Z., He, X., Sun, W., Chen, S., Wen, J., Gao, J., Wang, J., 2021.  
 1333 Evaluation of the ERA5 reanalysis precipitation dataset over Chinese Mainland. *J. Hy-*  
 1334 *drol.* 595, 125660. <https://doi.org/10.1016/j.jhydrol.2020.125660>
- 1335 Knoben, W.J.M., 2021. Global USDA-NRCS soil texture class map. <https://doi.org/10.4211/hs.1361509511e44ad>
- 1336 Kurtzer, G.M., Sochat, V., Bauer, M.W., 2017. Singularity: Scientific containers for mo-  
 1337 bility of compute. *PLOS ONE* 12, e0177459. <https://doi.org/10.1371/journal.pone.0177459>
- 1338 Lehner, B., Grill, G., 2013. Global river hydrography and network routing: baseline data  
 1339 and new approaches to study the world’s large river systems: GLOBAL RIVER HYDROG-  
 1340 RAPHY AND NETWORK ROUTING. *Hydrol. Process.* 27, 2171–2186. <https://doi.org/10.1002/hyp.9740>
- 1341 Lehner, B., Verdin, K., Jarvis, A., 2008. New Global Hydrography Derived From Space-  
 1342 borne Elevation Data. *Eos Trans. Am. Geophys. Union* 89, 93. <https://doi.org/10.1029/2008EO100001>
- 1343 Leonard, L., Duffy, C., 2016. Visualization workflows for level-12 HUC scales: Towards  
 1344 an expert system for watershed analysis in a distributed computing environment. *En-*  
 1345 *viron. Model. Softw.* 78, 163–178. <https://doi.org/10.1016/j.envsoft.2016.01.001>
- 1346 Leonard, L., Duffy, C.J., 2014. Automating data-model workflows at a level 12 HUC scale:  
 1347 Watershed modeling in a distributed computing environment. *Environ. Model. Softw.*  
 1348 61, 174–190. <https://doi.org/10.1016/j.envsoft.2014.07.015>
- 1349 Leonard, L., Duffy, C.J., 2013. Essential Terrestrial Variable data workflows for distributed  
 1350 water resources modeling. *Environ. Model. Softw.* 50, 85–96. <https://doi.org/10.1016/j.envsoft.2013.09.003>
- 1351 Liang, X., Lettenmaier, D.P., Wood, E.F., Burges, S.J., 1994. A simple hydrologically  
 1352 based model of land surface water and energy fluxes for general circulation models. *J.*  
 1353 *Geophys. Res.* 99, 14415–14428.
- 1354 Lin, P., Pan, M., Beck, H.E., Yang, Y., Yamazaki, D., Frasson, R., David, C.H., Durand,  
 1355 M., Pavelsky, T.M., Allen, G.H., Gleason, C.J., Wood, E.F., 2019. Global Reconstruc-  
 1356 tion of Naturalized River Flows at 2.94 Million Reaches. *Water Resour. Res.* 55, 6499–  
 1357 6516. <https://doi.org/10.1029/2019WR025287>
- 1358 McMillan, H.K., 2021. A review of hydrologic signatures and their applications. *WIREs*  
 1359 *Water* 8. <https://doi.org/10.1002/wat2.1499>
- 1360 Melsen, L.A., Torfs, P.J.J.F., Uijlenhoet, R., Teuling, A.J., 2017. Comment on “Most  
 1361 computational hydrology is not reproducible, so is it really science?” by Christopher Hut-  
 1362 ton et al.: REPRODUCING COMPUTATIONAL STUDIES. *Water Resour. Res.* 53,  
 1363 2568–2569. <https://doi.org/10.1002/2016WR020208>
- 1364 Messenger, M.L., Lehner, B., Grill, G., Nedeva, I., Schmitt, O., 2016. Estimating the vol-  
 1365 ume and age of water stored in global lakes using a geo-statistical approach. *Nat. Com-*  
 1366 *mun.* 7, 13603. <https://doi.org/10.1038/ncomms13603>
- 1367 Miles, B., Band, L.E., 2015. Ecohydrology Models without Borders?: Using Geospatial  
 1368 Web Services in EcohydroLib Workflows in the United States and Australia, in: Den-  
 1369 zer, R., Argent, R.M., Schimak, G., Hřebíček, J. (Eds.), *Environmental Software Sys-*  
 1370 *tems. Infrastructures, Services and Applications, IFIP Advances in Information and Com-*  
 1371 *munication Technology.* Springer International Publishing, Cham, pp. 311–320. [https://doi.org/10.1007/978-](https://doi.org/10.1007/978-3-319-15994-2_31)  
 1372 [3-319-15994-2\\_31](https://doi.org/10.1007/978-3-319-15994-2_31)

- 1373 Miles, B.C., 2014. SMALL-SCALE RESIDENTIAL STORMWATER MANAGEMENT  
1374 IN URBANIZED WATERSHEDS: A GEOINFORMATICS-DRIVEN ECOHYDROL-  
1375 OGY MODELING APPROACH. A dissertation submitted to the faculty at the Univer-  
1376 sity of North Carolina at Chapel Hill, Chapel Hill 2014.
- 1377 Minder, J.R., Mote, P.W., Lundquist, J.D., 2010. Surface temperature lapse rates over  
1378 complex terrain: Lessons from the Cascade Mountains. *J. Geophys. Res.* 115, D14122.  
1379 <https://doi.org/10.1029/2009JD013493>
- 1380 Mizukami, N., Clark, M.P., Gharari, S., Kluzek, E., Pan, M., Lin, P., Beck, H.E., Ya-  
1381 mazaki, D., 2021. A Vector-Based River Routing Model for Earth System Models: Par-  
1382 allelization and Global Applications. *J. Adv. Model. Earth Syst.* 13. <https://doi.org/10.1029/2020MS002434>
- 1383 Mizukami, N., Clark, M.P., Sampson, K., Nijssen, B., Mao, Y., McMillan, H., Viger, R.J.,  
1384 Markstrom, S.L., Hay, L.E., Woods, R., Arnold, J.R., Brekke, L.D., 2016. mizuRoute  
1385 version 1: a river network routing tool for a continental domain water resources appli-  
1386 cations. *Geosci. Model Dev.* 9, 2223–2238. <https://doi.org/10.5194/gmd-9-2223-2016>
- 1387 Mizukami, N., Rakovec, O., Newman, A.J., Clark, M.P., Wood, A.W., Gupta, H.V., Ku-  
1388 mar, R., 2019. On the choice of calibration metrics for “high-flow” estimation using hy-  
1389 drologic models. *Hydrol. Earth Syst. Sci.* 23, 2601–2614. [https://doi.org/10.5194/hess-](https://doi.org/10.5194/hess-23-2601-2019)  
1390 [23-2601-2019](https://doi.org/10.5194/hess-23-2601-2019)
- 1391 Murphy, A.H., 1988. Skill Scores Based on the Mean Square Error and Their Relation-  
1392 ships to the Correlation Coefficient. *Mon. WEATHER Rev.* 116, 2417–2424. [https://doi.org/10.1175/1520-](https://doi.org/10.1175/1520-0493(1988)116%3C2417:SSBOTM%3E2.0.CO;2)  
1393 [0493\(1988\)116%3C2417:SSBOTM%3E2.0.CO;2](https://doi.org/10.1175/1520-0493(1988)116%3C2417:SSBOTM%3E2.0.CO;2)
- 1394 Nash, J.E., Sutcliffe, J.V., 1970. River flow forecasting through conceptual models part  
1395 I — A discussion of principles. *J. Hydrol.* 10, 282–290. [https://doi.org/10.1016/0022-](https://doi.org/10.1016/0022-1694(70)90255-6)  
1396 [1694\(70\)90255-6](https://doi.org/10.1016/0022-1694(70)90255-6)
- 1397 NCAR Research Applications Laboratory, RAL, 2021. Noah-Multiparameterization Land  
1398 Surface Model (Noah-MP LSM) [WWW Document]. URL [https://ral.ucar.edu/solutions/products/noah-](https://ral.ucar.edu/solutions/products/noah-multiparameterization-land-surface-model-noah-mp-lsm)  
1399 [multiparameterization-land-surface-model-noah-mp-lsm](https://ral.ucar.edu/solutions/products/noah-multiparameterization-land-surface-model-noah-mp-lsm) (accessed 11.15.21).
- 1400 Olden, J.D., Poff, N.L., 2003. Redundancy and the choice of hydrologic indices for char-  
1401 acterizing streamflow regimes. *River Res. Appl.* 19, 101–121. <https://doi.org/10.1002/rra.700>
- 1402 Pechlivanidis, I.G., Jackson, B.M., McIntyre, N.R., Wheeler, H.S., 2011. Catchment scale  
1403 hydrological modelling: a review of model types, calibration approaches and uncertainty  
1404 analysis methods in the context of recent developments in technology and applications.  
1405 *Glob. NEST* 13, 193–214.
- 1406 Pietroniro, A., Fortin, V., Kouwen, N., Neal, C., Turcotte, R., Davison, B., Versegny, D.,  
1407 Soulis, E.D., Caldwell, R., Evora, N., Pellerin, P., 2007. Development of the MESH mod-  
1408 elling system for hydrological ensemble forecasting of the Laurentian Great Lakes at the  
1409 regional scale. *Hydrol. Earth Syst. Sci.* 11, 1279–1294. [https://doi.org/10.5194/hess-](https://doi.org/10.5194/hess-11-1279-2007)  
1410 [11-1279-2007](https://doi.org/10.5194/hess-11-1279-2007)
- 1411 Pushpalatha, R., Perrin, C., Moine, N.L., Andréassian, V., 2012. A review of efficiency  
1412 criteria suitable for evaluating low-flow simulations. *J. Hydrol.* 420–421, 171–182. [https://doi.org/10.1016/j.jhydrol.](https://doi.org/10.1016/j.jhydrol.2012.05.010)
- 1413 QGIS Development Team, 2021. QGIS Geographic Information System. QGIS Associ-  
1414 ation.
- 1415 Samaniego, L., Kumar, R., Attinger, S., 2010. Multiscale parameter regionalization of  
1416 a grid-based hydrologic model at the mesoscale. *Water Resour. Res.* 46, 1–25. [https://doi.org/10.1029/2008WR00](https://doi.org/10.1029/2008WR001250)
- 1417 Sandve, G.K., Nekrutenko, A., Taylor, J., Hovig, E., 2013. Ten Simple Rules for Repro-  
1418 ducible Computational Research. *PLoS Comput. Biol.* 9, e1003285. <https://doi.org/10.1371/journal.pcbi.1003285>

- 1419 Sazib, N.S., 2016. Physically Based Modeling of the Impacts of Climate Change on Stream-  
1420 flow Regime. <https://doi.org/10.26076/7BBE-E62D>
- 1421 Sen Gupta, A., Tarboton, D.G., Hummel, P., Brown, M.E., Habib, S., 2015. Integration  
1422 of an energy balance snowmelt model into an open source modeling framework. *Envi-  
1423 ron. Model. Softw.* 68, 205–218. <https://doi.org/10.1016/j.envsoft.2015.02.017>
- 1424 Slater, L.J., Thirel, G., Harrigan, S., Delaigue, O., Hurley, A., Khouakhi, A., Prosdociami,  
1425 I., Vitolo, C., Smith, K., 2019. Using R in hydrology: a review of recent developments  
1426 and future directions. *Hydrol. Earth Syst. Sci.* 23, 2939–2963. [https://doi.org/10.5194/hess-  
1427 23-2939-2019](https://doi.org/10.5194/hess-23-2939-2019)
- 1428 Stagge, J.H., Rosenberg, D.E., Abdallah, A.M., Akbar, H., Attallah, N.A., James, R.,  
1429 2019. Assessing data availability and research reproducibility in hydrology and water re-  
1430 sources. *Sci. Data* 6, 190030. <https://doi.org/10.1038/sdata.2019.30>
- 1431 Stodden, V., Miguez, S., 2013. Best Practices for Computational Science: Software In-  
1432 frastructure and Environments for Reproducible and Extensible Research. *SSRN Elec-  
1433 tron. J.* <https://doi.org/10.2139/ssrn.2322276>
- 1434 Sulla-Menashe, D., Friedl, M.A., 2018. User Guide to Collection 6 MODIS Land Cover  
1435 (MCD12Q1 andMCD12C1) Product (User Guide).
- 1436 Sulla-Menashe, D., Gray, J.M., Abercrombie, S.P., Friedl, M.A., 2019. Hierarchical map-  
1437 ping of annual global land cover 2001 to present: The MODIS Collection 6 Land Cover  
1438 product. *Remote Sens. Environ.* 222, 183–194. <https://doi.org/10.1016/j.rse.2018.12.013>
- 1439 Tadono, T., Nagai, H., Ishida, H., Oda, F., Naito, S., Minakawa, K., Iwamoto, H., 2016.  
1440 GENERATION OF THE 30 M-MESH GLOBAL DIGITAL SURFACE MODEL BY ALOS  
1441 PRISM. *ISPRS - Int. Arch. Photogramm. Remote Sens. Spat. Inf. Sci.* XLI-B4, 157–  
1442 162. <https://doi.org/10.5194/isprsarchives-XLI-B4-157-2016>
- 1443 Tang, G., Clark, M.P., Papalexiou, S.M., Ma, Z., Hong, Y., 2020. Have satellite precip-  
1444 itation products improved over last two decades? A comprehensive comparison of GPM  
1445 IMERG with nine satellite and reanalysis datasets. *Remote Sens. Environ.* 240, 111697.  
1446 <https://doi.org/10.1016/j.rse.2020.111697>
- 1447 Tarboton, D.G., Horsburgh, J.S., Maidment, D.R., Whiteaker, T., Zaslavsky, I., Piasecki,  
1448 M., Goodall, J., Valentine, D., Whitenack, T., 2009. Development of a community hy-  
1449 drologic information system. Presented at the 18th World IMACS Congress and MOD-  
1450 SIM09 International Congress on Modelling and Simulation, Modelling and Simulation  
1451 Society of Australia and New Zealand and International Association for Mathematics  
1452 and Computers in Simulation, pp. 988–994.
- 1453 Tesfa, T.K., Tarboton, D.G., Watson, D.W., Schreuders, K.A.T., Baker, M.E., Wallace,  
1454 R.M., 2011. Extraction of hydrological proximity measures from DEMs using parallel  
1455 processing. *Environ. Model. Softw.* 26, 1696–1709. <https://doi.org/10.1016/j.envsoft.2011.07.018>
- 1456 Tiesinga, E., Mohr, P.J., Newell, D.B., Taylor, B.N., 2019. The 2018 CODATA Recom-  
1457 mended Values of the Fundamental Physical Constants. National Institute of Standards  
1458 and Technology, Gaithersburg, MD 20899.
- 1459 U.S. Department of Agriculture: Agricultural Research Service (USDA ARS), 2021. ROSETTA  
1460 Class Average Hydraulic Parameters [WWW Document]. URL [https://www.ars.usda.gov/pacific-  
1461 west-area/riverside-ca/agricultural-water-efficiency-and-salinity-research-unit/docs/model/rosetta-  
1462 class-average-hydraulic-parameters/](https://www.ars.usda.gov/pacific-west-area/riverside-ca/agricultural-water-efficiency-and-salinity-research-unit/docs/model/rosetta-class-average-hydraulic-parameters/) (accessed 11.15.21).
- 1463 Vanderborght, J., Kasteel, R., Herbst, M., Javaux, M., Thiéry, D., Vanclooster, M., Mou-  
1464 vet, C., Vereecken, H., 2005. A Set of Analytical Benchmarks to Test Numerical Mod-  
1465 els of Flow and Transport in Soils. *Vadose Zone J.* 4, 206. <https://doi.org/10.2136/vzj2005.0206>

- 1466 Vorobeuskii, I., Kronenberg, R., Bernhofer, C., 2020. Global BROOK90 R Package: An  
1467 Automatic Framework to Simulate the Water Balance at Any Location. *Water* 12, 2037.  
1468 <https://doi.org/10.3390/w12072037>
- 1469 Wallace, J.M., Hobbs, P.V., 2006. *Atmospheric science: an introductory survey*, 2nd ed.  
1470 ed, International geophysics series. Elsevier Academic Press, Amsterdam ; Boston.
- 1471 Weiler, M., Beven, K., 2015. Do we need a community hydrological model? *Water Re-*  
1472 *sour. Res.* 51. <https://doi.org/10.1002/2014WR016731>
- 1473 Wilkinson, M.D., Dumontier, M., Aalbersberg, I.J., Appleton, G., Axton, M., Baak, A.,  
1474 Blomberg, N., Boiten, J.-W., da Silva Santos, L.B., Bourne, P.E., Bouwman, J., Brookes,  
1475 A.J., Clark, T., Crosas, M., Dillo, I., Dumon, O., Edmunds, S., Evelo, C.T., Finkers, R.,  
1476 Gonzalez-Beltran, A., Gray, A.J.G., Groth, P., Goble, C., Grethe, J.S., Heringa, J., 't  
1477 Hoen, P.A.C., Hoofst, R., Kuhn, T., Kok, R., Kok, J., Lusher, S.J., Martone, M.E., Mons,  
1478 A., Packer, A.L., Persson, B., Rocca-Serra, P., Roos, M., van Schaik, R., Sansone, S.-  
1479 A., Schultes, E., Sengstag, T., Slater, T., Strawn, G., Swertz, M.A., Thompson, M., van  
1480 der Lei, J., van Mulligen, E., Velterop, J., Waagmeester, A., Wittenburg, P., Wolsten-  
1481 croft, K., Zhao, J., Mons, B., 2016. The FAIR Guiding Principles for scientific data man-  
1482 agement and stewardship. *Sci. Data* 3, 160018. <https://doi.org/10.1038/sdata.2016.18>
- 1483 Xu, X., Frey, S.K., Boluwade, A., Erler, A.R., Khader, O., Lapen, D.R., Sudicky, E., 2019.  
1484 Evaluation of variability among different precipitation products in the Northern Great  
1485 Plains. *J. Hydrol. Reg. Stud.* 24, 100608. <https://doi.org/10.1016/j.ejrh.2019.100608>
- 1486 Yamazaki, D., Ikeshima, D., Sosa, J., Bates, P.D., Allen, G.H., Pavelsky, T.M., 2019. MERIT  
1487 Hydro: A High-Resolution Global Hydrography Map Based on Latest Topography Dataset.  
1488 *Water Resour. Res.* 55, 5053–5073. <https://doi.org/10.1029/2019WR024873>
- 1489 Yamazaki, D., Ikeshima, D., Tawatari, R., Yamaguchi, T., O'Loughlin, F., Neal, J.C.,  
1490 Sampson, C.C., Kanae, S., Bates, P.D., 2017. A high-accuracy map of global terrain el-  
1491 evations: Accurate Global Terrain Elevation map. *Geophys. Res. Lett.* 44, 5844–5853.  
1492 <https://doi.org/10.1002/2017GL072874>